View metadata, citation and similar papers at core.ac.uk

brought to you by CORE

provided by Digital Repository @ Iowa State University

IOWA STATE UNIVERSITY
Digital Repository

Retrospective Theses and Dissertations

Iowa State University Capstones, Theses and Dissertations

1969

An application of Regge theory and SU(3) representation mixing to high energy reactions suggesting a second A2 meson

Donald Murray Austin
Iowa State University

Follow this and additional works at: https://lib.dr.iastate.edu/rtd


Part of the Nuclear Commons

Recommended Citation

Austin, Donald Murray, "An application of Regge theory and SU(3) representation mixing to high energy reactions suggesting a second A2 meson " (1969). *Retrospective Theses and Dissertations*. 3555.
https://lib.dr.iastate.edu/rtd/3555

This Dissertation is brought to you for free and open access by the Iowa State University Capstones, Theses and Dissertations at Iowa State University Digital Repository. It has been accepted for inclusion in Retrospective Theses and Dissertations by an authorized administrator of Iowa State University Digital Repository. For more information, please contact digirep@iastate.edu.

This dissertation has been
microfilmed exactly as received

69-20,621

AUSTIN, Donald Murray, 1938-

AN APPLICATION OF REGGE THEORY AND SU(3) REPRESENTATION MIXING TO HIGH ENERGY REACTIONS SUGGESTING A SECOND A_2 MESON.

Iowa State University, Ph.D., 1969
Physics, nuclear

University Microfilms, Inc., Ann Arbor, Michigan

AN APPLICATION OF REGGE THEORY AND SU(3) REPRESENTATION MIXING TO HIGH ENERGY REACTIONS SUGGESTING A SECOND A_2 MESON

by

Donald Murray Austin

A Dissertation Submitted to the
Graduate Faculty in Partial Fulfillment of
The Requirements for the Degree of
DOCTOR OF PHILOSOPHY

Major Subject: Physics

Approved:

Signature was redacted for privacy.
In Charge of Major Work

Signature was redacted for privacy.
Head of Major Department

Signature was redacted for privacy.
Dean of Graduate College

Iowa State University
Of Science and Technology
Ames, Iowa

1969

TABLE OF CONTENTS

I. INTRODUCTION

The development of theoretical high energy physics, or elementary particle physics, has proceeded largely through the phenomenological approach. This approach consists of exploiting as fully as possible several broadly accepted principles of high energy reactions, such as analyticity and unitarity of the scattering amplitude or unitary symmetry of the observed particle states, and determining the parameters not specified by the general principles by numerically fitting experimental data. Models based on the apparent SU(3) symmetry of the observed mesons and baryons, and the Regge model, based on analyticity of scattering amplitudes in the Mandelstam variables, have been the most successful of the phenomenological theories applied to the ever-growing list of "elementary" particles observed by experimental groups working with high energy accelerators. Among the successes of the SU(3) model, and unitary symmetry in general, are the classification of over a hundred observed "particles" into well defined singlets, octets and decuplets related to each other by the known properties of the group, and the accurate prediction of certain constants of the theory, such as baryon magnetic moment ratios and coupling constants. The Regge theory, on the other hand, has been successful in predicting the correct energy dependence of high energy cross sections and polarization measurements, as well as relating the various particle multiplets to others with higher spins and masses. In view of the impressive successes these theories have had in predicting and explaining huge quantities of data, the appearance of several rather drastic contradictions between theory and experiment in a few reactions

serves to stimulate further refinements of these theories, sometimes even suggesting new fields of interest to the experimentalist. It is the purpose of this dissertation to deal with three such instances in which small changes in the previously adequate theory are made in order to explain some anomalies seen in recent experiments. These anomalies are the twin-peaked A_2 mass distribution seen by several independent experimental groups, the possible non-zero polarization of the neutron seen in eta production in pion-proton scattering, and the large forward peak seen in charged pion photoproduction. In each instance it is found that the data can be easily explained by introducing a second A_2-type meson belonging to an SU(3) multiplet different from the octet with which the usual A_2 tensor meson is associated. A simple interpretation of this new meson multiplet is given in terms of the quark model, and the properties of the SU(3) symmetry group are used to determine relations between the relevant coupling constants. Good fits to the aforementioned data are obtained by applying the concept of representation mixing, developed here in a field-theoretic framework. Also, some further consequences of the theory are examined. In particular, the application of the theory to the duality hypothesis, in which a bootstrap mechanism serves to relate Regge poles in the crossed channel to direct channel resonances, is carried out for an inelastic reaction and compared with analyses of the elastic reaction.

In Chapter II, an SU(3) representation mixing formalism is developed in the framework of LSZ field theory which allows a simple and direct interpretation of the mixing of particle states by means of a non-diagonal mass matrix assumed to be generated by an SU(3)-breaking interaction. This formalism is applied to the twin-peaked A_2 mass distribution in

Chapter III, and the best fit parameters for the masses, decay widths and mixing angles are obtained for two different interpretations of recent experiments. In Chapter IV the scattering amplitudes obtained from the mixing theory are Reggeized and used in fitting the cross sections and polarization measurements for eta production in pion-proton scattering[a]. The relation of the Regge parameters thus obtained to those required to explain the forward peak in pion photoproduction is also discussed in this chapter. A partial wave analysis of the Regge amplitudes is carried out in Chapter V, and Argand diagrams (plots of the real part of the scattering amplitude versus the imaginary part) are obtained. By applying the accepted criterion for the existence of a resonance state, we find that a series of direct channel baryonic resonances is generated by the t-channel exchange of mesonic Regge trajectories. These resonances are compared to those seen in a similar analysis of pion-proton elastic and charge exchange scattering and in a recent phase shift analysis of the low energy data for the same reaction. Derivation of a suitable form of the scattering amplitudes required here is carried out in Appendix A, the Reggeization procedure and the various ghost-killing mechanisms are discussed in Appendix B, and a general form for the inelastic scattering matrix element and its associated Argand diagram is derived in Appendix C.

[a]The phrase "eta production in pion-proton scattering" has been shortened to "eta pion-production" in the remainder of the text.

II. SU(3) REPRESENTATION MIXING IN A FIELD-THEORETIC FRAMEWORK

A. Introduction

Unitary symmetry of particle states can be viewed as an extension of isospin symmetry, represented by SU(2), to a higher order unitary group (1). The existence of a new quantum number called "strangeness" led to the hypothesis that particle states would, in the presence of only a superstrong force, carry irreducible representations of the Lie group SU(3). The mass degeneracy is removed by an SU(3)-breaking interaction, just as the electromagnetic interaction breaks the isospin symmetry. This analogy with quantum electrodynamics is perhaps most handily exploited in terms of second-quantized relativistic field theory (2), where the field operators can be thought of as carrying the group representations, and the interactions enter through the field equations. This is by no means the only formalism in which the symmetry properties of observed particle states can be exploited, but it does offer at least a complete notational system in which the interpretation of the particles and their interactions can be easily understood. We shall not be concerned here with the more intricate problems of quantum field theory, but simply use the field concepts as a basis for the notation.

When introducing an SU(3)-breaking interaction to account for the mass splitting among the particles in a given multiplet, Gell-Mann and Okubo (1) observe that in order to obtain a good fit to measured masses of the particles involved, the singlet and octet states with zero isospin must be considered to exist as physical states which are mixtures of the basis states for the group multiplet. Since these states have exactly the same internal quantum numbers (spin, isospin, parity and charge

conjugation) except for their SU(3) representation labels, the symmetry breaking interaction allows physical states to occur as linear combinations of the SU(3) states. This singlet-octet mixing of the isospin zero components is seen to occur in all the known nonets (singlet + octet) observed thus far, and the theoretical predictions of the mixing theory are well borne out by the data.

In this chapter a general mixing formalism is developed in the framework of LSZ field theory (2). The case of scalar fields is treated first, and then the formalism is extended to higher spin boson fields by use of a projection operator technique. The effects of field renormalization are included in the result insofar as the pole approximation for the propagator function is valid.

B. Mixing of Scalar Fields

Consider two scalar fields, φ_1 and φ_2, each of which carries an irreducible representation of SU(3). These fields are taken to satisfy a matrix Klein-Gordon equation with an SU(3)-breaking interaction which causes the fields to be mixed. Forming a two-vector $\vec{\varphi}$, we can write the equation satisfied by these fields in the form

$$(\Box^2 \underset{\sim}{1} + \underset{\sim}{M}_g^2) \vec{\varphi}(x) = \vec{j}(x) \qquad (2.1)$$

where

$$\vec{\varphi}(x) = \begin{pmatrix} \varphi_1(x) \\ \varphi_2(x) \end{pmatrix} , \quad \vec{j}(x) = \begin{pmatrix} j_1(x) \\ j_2(x) \end{pmatrix} ,$$

and

$$\underset{\sim}{M}_g^2 = \begin{pmatrix} M_1^2 & M_{12}^2 \\ M_{12}^2 & M_2^2 \end{pmatrix} .$$

The mass matrix $\underset{\sim}{M}_g^2$ includes the mixing of the interacting fields. Assuming that the mass matrix has nondegenerate eigenvalues, we make a unitary transformation of the wave equation 2.1 which diagonalizes the mass matrix,

$$\underset{\sim}{U}\,(\Box^2\,\underset{\sim}{1} + \underset{\sim}{M}_g^2)\,\underset{\sim}{U}^\dagger\,\underset{\sim}{U}\,\vec{\varphi}\,(x) = (\Box^2\,\underset{\sim}{1} + \underset{\sim}{M}^2)\,\vec{\Psi}(x) = \underset{\sim}{U}\,\vec{j}(x) = \vec{j}'(x), \tag{2.2}$$

where

$$\vec{\Psi}(x) = \underset{\sim}{U}\,\vec{\varphi}\,(x),$$

$$\vec{j}'(x) = \underset{\sim}{U}\,\vec{j}\,(x),$$

and

$$\underset{\sim}{M}^2 = \underset{\sim}{U}\,\underset{\sim}{M}_g^2\,\underset{\sim}{U}^{-1} = \begin{pmatrix} m_1^2 & 0 \\ 0 & m_2^2 \end{pmatrix}. \tag{2.3}$$

The m_i^2 are the masses of the states corresponding to the interpolating fields Ψ_i. Since the equations for the fields are now separated, the free fields required to construct physical single-particle states from the vacuum can be formed by taking a suitable functional of the physical fields and their currents. The free fields, denoted by Ψ^{in}_i, are defined to have the following properties:

a. $\Psi^{in}_i(x)$ transforms under the Poincaré group in the same way as the $\Psi_i(x)$. In particular,
$[P^\mu, \Psi^{in}_i(x)] = -i\,\frac{\partial}{\partial x_\mu}\,\Psi^{in}_i(x)$.

b. The space-time development of $\Psi^{in}_i(x)$ is described by a Klein-Gordon equation with physical masses m'^2_i,
$(\Box^2\,\underset{\sim}{1} + \underset{\sim}{M}_o^2)\,\vec{\Psi}^{in}(x) = 0$,
$\underset{\sim}{M}_o^2 = \begin{pmatrix} m_1'^2 & 0 \\ 0 & m_2'^2 \end{pmatrix}$.

The $\Psi^{in}_i(x)$ fields create physical one-particle states from the vacuum, as can be seen by noting that

$$-i\partial^\mu \langle 0 | \Psi^{in}_i(x) | n \rangle = \langle 0 | [P^\mu, \Psi^{in}_i(x)] | n \rangle$$
$$= p_n{}^\mu \langle 0 | \Psi^{in}_i(x) | 0 \rangle,$$
$$-\partial_\mu \partial^\mu \langle 0 | \Psi^{in}_i(x) | n \rangle = - p_n{}^\mu p_{n\mu} \langle 0 | \Psi^{in}_i(x) | n \rangle .$$

Hence,

$$(\Box^2 + m_i{}^2) \langle 0 | \Psi^{in}_i(x) | n \rangle = (m_i^2 - p_n{}^2) \langle 0 | \Psi^{in}_i(x) | n \rangle = 0,$$

so that the only states produced from the vacuum by $\Psi^{in}_i(x)$ are single-particle states of mass m_i^2.

The free fields have the usual Fourier expansion in terms of the creation and destruction operators in momentum space,

$$\Psi^{in}_i(x) = \int d^3p \{ a^{in}_i(p) f_p(x) + b^{in}_i{}^\dagger(p) f_p{}^*(x) \},$$

where

$$f_p(x) = (2\pi)^{-3/2} (2E_p)^{-1/2} e^{-ip\cdot x},$$

$$E_p = (p^2 + m^2)^{1/2} = p^o,$$

$a^{in}_i(p)$ = destruction operator for a free state i with momentum p, and

$b^{in}_i{}^\dagger(p)$ = creation operator for a free antiparticle state i with momentum p.

For a charged scalar field, $a^{in}_i = a_+{}^{in}_i$ and $b^{in}_i{}^\dagger = a_-{}^{in}_i{}^\dagger$.

In order to relate the free fields to the interpolating fields, we introduce a mass counterterm into the Klein-Gordon equation 2.2 in the following manner:

$$(\Box^2 + m_i{}^2) \Psi_i(x) = j'_i(x) + (m'_i{}^2 - m'_i{}^2) \Psi_i(x),$$
$$(\Box^2 + m'_i{}^2) \Psi_i(x) = j'_i(x) + (m'_i{}^2 - m_i{}^2) \Psi_i(x) \equiv j''_i(x).$$

The current $j''_i(x)$ is treated as the source giving rise to the scattered waves which are present in addition to the free waves $\Psi^{in}_i(x)$ propagating with mass m'_i. This suggests the functional relation between the free fields and the interpolating fields and current,

$$\sqrt{Z_i}\ \Psi^{in}_i(x) = \Psi_i(x) - \int d^4y\ \Delta_{ret}(x-y;\ m_i^2)\ j''_i(y), \tag{2.4}$$

where

$$\Delta_{ret}(x-y;\ m_i^2) = 0 \text{ for } x_o < y_o,$$

$$(\Box^2 + m_i^2)\ \Delta_{ret}(x-y;\ m_i^2) = \delta^4(x - y),$$

and Z_i is the renormalization constant. Since the current $j''_i(x)$ is a scalar operator, it is easy to show that this definition of the free field $\Psi^{in}_i(x)$ satisfies the two conditions a and b on page 6. The renormalization constant Z_i is included to permit normalization of the matrix element for the free field to create one-particle states from the vacuum to unit amplitude. The correct asymptotic condition relating the fields, the Lehmann, Symanzik, Zimmermann (LSZ) weak convergence limit (2), is obtained by smearing the fields over a space-like region according to

$$\Psi^f(t) = i\int d^3x\ f^*(x,t)\ \overleftrightarrow{\partial}_o\ \Psi(x,t),$$

where $f(x,t)$ is an arbitrary normalizable solution to the homogeneous Klein-Gordon equation. Taking any two normalizable states $|\alpha\rangle$ and $|\beta\rangle$, we obtain the LSZ asymptotic condition

$$\lim_{t\to-\infty} \langle\alpha|\ \Psi^f(t)\ |\beta\rangle = \sqrt{Z}\ \langle\alpha|\ \Psi^f_{in}\ |\beta\rangle,$$

and Ψ^f_{in}, defined analogously to $\Psi^f(t)$, is independent of time. The spectral representation of the Feynman propagator for the free fields is given by

$$\Delta^{o}_{ij}(x,y) \equiv -i\langle 0|T\{\Psi^{in}_{i}(x)\ \Psi^{in}_{j}{}^{\dagger}(y)\}|0\rangle \qquad (2.5)$$

$$= -i(2\pi)^{-3}\int d^4q\ \rho^{o}_{ij}(q)\ \{\Theta(x_o-y_o)\ e^{-iq\cdot(x-y)}$$

$$+\Theta(y_o-x_o)\ e^{+iq\cdot(x-y)}\ \}$$

$$= \int_0^\infty \rho^{o}_{ij}(m^2)\ \Delta_F{}^{o}(x-y;\ m^2)\ dm^2\ ,$$

where

$$\rho^{o}_{ij}(q) \equiv (2\pi)^3 \sum_n \delta^4(p_n-q)\ \langle 0|\ \Psi^{in}_{i}(0)|n\rangle\langle n|\Psi^{in}_{j}{}^{\dagger}(0)|0\rangle$$

$$=\rho^{o}_{ji}{}^{*}(q)$$

$$=\rho^{o}_{ij}(q^2)\ \Theta(q^o),$$

and

$$\Delta_F{}^{o}(x-y;\ m^2) \equiv -i(2\pi)^3\int d^4q\ \delta(q^2-m^2)[\Theta(x_o-y_o)\ e^{-iq\cdot(x-y)}$$

$$+\Theta(y_o-x_o)\ e^{+iq\cdot(x-y)}]$$

is the usual Feynman propagator. In momentum space the free field propagator becomes

$$\Delta^{o}_{ij}(p) = \int_o^\infty dm^2\ \rho^{o}_{ij}(m^2)\ (p^2 - m^2 + i\epsilon)^{-1}. \qquad (2.6)$$

From the definition of the free fields, we obtain

$$\langle 0|\psi^{in}_{i}(x)\ |n\rangle = f_{p_n}(x)\ \delta_{i,n}\ , \qquad (2.7)$$

where $f_{p_n}(x)$ is a solution to the homogeneous Klein-Gordon equation,

$$f_{p_n}(x) = [(2\pi)^3\ 2\ E_p]^{-1/2}\ e^{-ip_n\cdot x}\ .$$

With this expression inserted into the expression for the free field spectral function 2.5, the propagator for two free particles becomes

$$\underset{\sim}{\Delta}^{o}(p) = \left\{ \begin{array}{cc} \dfrac{1}{p^2 - m'_1{}^2 + i\epsilon} & 0 \\ 0 & \dfrac{1}{p^2 - im'_2{}^2 + i\epsilon} \end{array} \right\} \tag{2.8}$$

$$= (p^2 \underset{\sim}{1} - \underset{\sim}{M}_o{}^2)^{-1},$$

where the $m'_i{}^2$ are the masses of the physical states. The propagator for the interpolating fields ψ_i is defined analogously to that for the free fields,

$$\rho_{ij}(q) \equiv \sum_n \delta^4(p_n - q) \langle 0|\psi_i(0)|n\rangle\langle n|\psi_j^{\dagger}(0)|0\rangle, \tag{2.9}$$

which gives, for ρ real and timelike,

$$\Delta'_{ij}(x-y) \equiv -i \langle 0|T\{\psi_i(x)\ \psi_j^{\dagger}(y)\}|0\rangle \tag{2.10}$$

$$= \int_o^{\infty} dm^2\ \rho_{ij}(m^2)\ \Delta_F(x-y;\ m^2),$$

$$\Delta'_{ij}(p) = \int_o^{\infty} dm^2\ \rho_{ij}(m^2)\ (p^2 - m^2 + i\epsilon)^{-1}.$$

The pole approximation (3) consists of taking the sum in 2.9 over the physical single-particle states only. Using 2.4 and 2.7, we obtain

$$\underset{\sim}{\Delta}'(p) = \underset{\sim}{Z}^{1/2}\ \underset{\sim}{\Delta}^{o}(p)\ \underset{\sim}{Z}^{1/2} + \int_{\mu^2}^{\infty} dm^2\ \underset{\sim}{\rho}(m^2)\ \Delta_F(p;\ m^2) \tag{2.11}$$

where the first part is the pole term and the second part is the integral of the spectral function times the Feynman propagator over the continuum. Here $(\underset{\sim}{Z}^{1/2})_{ij} \equiv \sqrt{Z_i}\ \delta_{ij}$, and μ^2 is the two-particle intermediate state threshold. Thus far we have been dealing with stable particles, since the existence of the free fields implies the LSZ weak convergence limit as $t \to \pm\infty$. To generalize the formalism to include unstable particles, one can either take the approach of Coleman and Schnitzer (3), which is

to take the pole approximation and let the masses become complex, or one can drop the pole term and assume that the spectral function contains a Breit-Wigner type of mass distribution, so that the integral over the continuum gives a propagator with complex masses. In either case we obtain a propagator with poles on the unphysical sheet of the complex p^2 plane,

$$\underset{\sim}{\Delta}'(p) = \underset{\sim}{Z}^{1/2} (p^2 \underset{\sim}{1} - \underset{\sim}{M}_o^2)^{-1} \underset{\sim}{Z}^{1/2} , \tag{2.12}$$

where now the elements of $\underset{\sim}{M}^2$ have the form $m_i^2 - im_i\gamma_i$, and the γ_i are the decay widths of the resonances. The propagator for the unmixed SU(3) fields, φ_i, is given by

$$\begin{aligned} \Delta'^{g}_{ij}(x-y) &\equiv -i \langle 0|T\{\varphi_i(x)\, \varphi_j^{\dagger}(y)\}|0\rangle \\ &= -i \langle 0|T\{U^{-1}_{ik}\, \Psi_k(x)\, \Psi_l^{\dagger}(y)\, U^{\dagger -1}_{lj}\}|0\rangle \\ &= U^{-1}_{ik}\, \Delta'_{kl}(x-y)\, U_{lj}, \end{aligned} \tag{2.13}$$

with

$$\underset{\sim}{M}_g^2 = \underset{\sim}{U}^{-1}\, \underset{\sim}{M}_o^2\, \underset{\sim}{U}, \tag{2.14}$$

and the elements of $\underset{\sim}{M}_g^2$ are now complex.

C. The S-Matrix in Terms of the SU(3) Fields

Consider the S-matrix element for scattering from some initial two-particle state $|\alpha_{in}\rangle$ to some two-particle final state $|\beta_{out}\rangle$ mediated by the interpolating fields Ψ_i by means of an interaction linear in the fields

$$H_I = \vec{j}_{\beta}^{\dagger} \cdot \vec{\Psi} + \vec{\Psi}^{\dagger} \cdot \vec{j}_{\alpha} \ . \tag{2.15}$$

For example, a scalar interaction may be written in the form

$$\vec{j}^{\dagger}_{\alpha} \cdot \vec{\Psi} = \Phi_{\alpha}^{\dagger}\, \vec{\alpha}^{\dagger} \cdot \vec{\Psi} = \Phi_{\alpha}^{\dagger} (\alpha_1 \Psi_1 + \alpha_2 \Psi_2),$$

where $\Phi_\alpha^\dagger \alpha_i \Psi_i$ is the interaction determining the decay of the Ψ_i into the two-particle state $\Phi_\alpha^\dagger|0\rangle \equiv |\alpha\rangle$, with form factor α_i. Here we are treating the two-body initial and final states only symbolically since our main purpose is to investigate the form of the propagator of the interpolating fields Ψ_i and φ_i. Carrying out the usual procedures for the reduction of the S-matrix (2), we obtain

$$S_{\beta\alpha} \equiv \langle \beta_{out}, p_f | \alpha_{in}, p_i \rangle \tag{2.16}$$
$$= \delta_{\beta\alpha} + i^2 \int d^4y d^4x \{ f_{p_f}^{\beta}(x) K_x \tau_{\beta\alpha}(x,y) K_y f_{p_i}^{\alpha *}(y) \},$$

where $K_x = \Box_x^2 + m_\beta^2$ and $K_y = \Box_y^2 + m_\alpha^2$ operate only on the τ-function, which is given, to second order in H_1, by

$$\tau_{\beta\alpha}(x,y) = \langle 0|T\{\Phi_\beta(x)\ \Phi_\alpha^\dagger(y)\}|0\rangle \tag{2.17}$$
$$= (-i)^2 \int d^4y_1 d^4x_1 \{ [iD_\beta(x-x_1)][i\vec{\beta}\cdot\underset{\sim}{\Delta}^o(x_1-y_1)\cdot\vec{\alpha}][iD_\alpha(y_1-y)] \},$$

where

$$iD_\beta(x-x_1) \equiv \langle 0|T\{\Phi^{in}_\beta(x)\ j^{in\,\dagger}_\beta(x_1)\}|0\rangle,$$

$$K_x \cdot D_\beta(x-x_1) = \delta^4(x-x_1),$$

and similarly for $D_\alpha(y-y_1)$. In momentum space, the S-matrix takes the form

$$S_{\beta\alpha}(p_f,p_i) = \delta_{\beta\alpha} - (2\pi)^4 i\ \rho_\alpha^{-1} \rho_\beta^{-1}\ \delta^4(p_f-p_i)\ \{\vec{\beta}\cdot\underset{\sim}{\Delta}^o(t)\cdot\vec{\alpha}\}, \tag{2.18}$$

where t is the four-momentum transfer and ρ_α, ρ_β are the densities of states for the initial and final two-body states. The T-matrix is defined

$$T_{\beta\alpha}(p_f,p_i) \equiv \vec{\beta}\cdot\underset{\sim}{\Delta}^o(t)\cdot\vec{\alpha}. \tag{2.19}$$

The coupling of the states $|\alpha\rangle$ and $|\beta\rangle$ to the unmixed fields is given by

$$H_i = j_\beta^\dagger\ \vec{\beta}^\dagger \cdot \underset{\sim}{U}\ \vec{\varphi} + \vec{\varphi}^\dagger\ \underset{\sim}{U}^\dagger \cdot \vec{\alpha}\ j_\alpha \tag{2.20}$$

$$= j_\beta^\dagger \vec{\beta}^\dagger{}_g \cdot \vec{\varphi} + \vec{\varphi}^\dagger \cdot \vec{\alpha}_g \, j_\alpha,$$

where

$$\vec{\alpha}_g \equiv \underset{\sim}{U}^\dagger \vec{\alpha}, \tag{2.21}$$

and

$$\vec{\beta}_g^\dagger \equiv \vec{\beta}^\dagger \underset{\sim}{U}.$$

In terms of the mass matrix $\underset{\sim}{M}_g^2$, the T-matrix becomes

$$T_{\beta\alpha} = \vec{\beta}^\dagger \cdot (t \underset{\sim}{1} - \underset{\sim}{M}_o^2)^{-1} \cdot \vec{\alpha} \tag{2.22}$$

$$= \vec{\beta}^\dagger \cdot \underset{\sim}{Z}^{-1/2} \underset{\sim}{U} \underset{\sim}{\Delta}'_g(t) \underset{\sim}{U}^{-1} \underset{\sim}{Z}^{-1/2} \cdot \vec{\alpha}$$

$$= \vec{\beta}_g^\dagger \cdot (t \underset{\sim}{1} - \underset{\sim}{M}_g^2)^{-1} \cdot \vec{\alpha}_g,$$

where 2.12 - 2.14 have been used. Here $\vec{\alpha}_g$ and $\vec{\beta}_g$ are the SU(3) coupling constants (unrenormalized). The coupling constants are considered to exhibit SU(3) symmetry in the sense that the production and decay amplitudes for the "particles" corresponding to the φ_i fields into the states $|\alpha\rangle$ and $|\beta\rangle$ carrying representations of SU(3) are products of SU(3) Clebsch-Gordan coefficients and reduced matrix elements.

D. Mixing of Boson Fields with Spin

The formalism developed by Rivers (4) for propagators of spin j fields associates with the spectral function a projection operator $P_{(\mu)(\gamma)}(p)$, $(\mu) = \mu_1, \mu_2, \ldots \mu_j$, which is the sum of products of the spin 1 projection operator,

$$P_{1\mu\gamma} = g_{\mu\gamma} - p_\mu p_\gamma / p^2.$$

The free fields are defined by the Fourier decomposition

$$\Psi^{in}_{i(\mu)}(x) \equiv \int d^3p \sum_\lambda e_{(\mu)}^{(\lambda)}(p) \{ a_+^{(\lambda)}(p) \, f_p(x) + a_-^{\dagger(\lambda)}(p) \, f_p^*(x) \} \tag{2.23}$$

where

$$[a_+^{in(\lambda)}{}_i(p),\ a_+^{in(\lambda')}{}_j^{\dagger}(p')] = \delta_{ij}\delta_{\lambda\lambda'}\,\delta^3(\vec{p}-\vec{p}'),$$

$$\sum_\lambda e_{(\mu)}^{(\lambda)}(p)\ e_{(\gamma)}^{(\lambda)}(p) \equiv P_{(\mu)(\gamma)}(p),$$

$(\mu) = \mu_1,\mu_2,\ldots,\mu_j$, for $\mu_i = 1,2,3,0$,

$(\lambda) = \lambda_1,\lambda_2,\ldots,\lambda_i$, for $\lambda_i = 1,2,\ldots,2j+1$,

and $P_{(\mu)(\gamma)}(p)$ is the sum of products of the spin 1 projection operator.

The free field spectral function is defined by

$$\rho^o{}_{(\mu)(\gamma)}^{ij}(p) \equiv \sum_n \delta^4(p_n-p)\langle 0|\ \Psi^{in}{}_{(\mu)}^{i}(0)|n\rangle\langle n|\Psi^{in}{}_{(\gamma)}^{j\dagger}(0)|0\rangle. \tag{2.24}$$

Taking $\sum_n \to \sum_{r=1}^{2} \int d^3p_n \sum_\lambda$ to define the sum over intermediate states, we obtain

$$\begin{aligned}\rho^o{}_{(\mu)(\gamma)}^{ij}(p) &= \sum_r \int d^3p_n \delta^4(p_n-p) f_{p_n}(0)\delta^i{}_r \sum_\lambda e_{(\mu)}^{(\lambda)}(p_n) e_{(\gamma)}^{(\lambda)}(p_n)\delta_{rj} f_{p_n}^{*}(0)\\ &= \sum_r \delta_{ir}\delta_{rj}\delta(p^2 - m_r^2)\ P_{(\mu)(\gamma)}(p)\ \Theta(p^o)\\ &= P_{(\mu)(\gamma)}(p)\ \rho^{oij}(p^2)\ \Theta(p^o),\end{aligned}$$

where

$$\rho^{0ij}(p^2) = \sum_r \delta_{ir}\delta_{rj}\ \delta(p^2-m_r^2),$$

just as we had for the scalar fields. This leads to a spin j propagator

$$\Delta^o{}_{(\mu)(\gamma)}^{ij}(x,y) \equiv -i\langle 0|T\{\Psi^{in}{}_{(\mu)}^{i}(x)\ \Psi^{in}{}_{(\gamma)}^{j\dagger}(y)\}|0\rangle \tag{2.25}$$

$$\begin{aligned}&= -i\int d^4p\ \rho^o{}_{(\mu)(\gamma)}^{ij}(p)\ \{\Theta(x_o-y_o)\ e^{-ip\cdot(x-y)}\\ &\qquad\qquad +\Theta(y_o-x_o)\ e^{+ip\cdot(x-y)}\}\\ &= \int_o^\infty dm^2\ \rho^{oij}(m^2)\ \Delta_{F(\mu)(\gamma)}(x-y;\ m^2),\end{aligned}$$

where

$$\Delta_{F(\mu)(\gamma)}(x-y;\, m^2) \equiv -i\int d^4p\,\delta(p^2-m^2)\Theta(p^o)\,P_{(\mu)(\gamma)}(p)\{\Theta(x_o-y_o)e^{-ip\cdot(x-y)} + \Theta(y_o-x_o)e^{+ip\cdot(x-y)}\},$$

the Feynman propagator for spin j fields. The Feynman propagator in momentum space is

$$\Delta_{F(\mu)(\gamma)}(p;\, m^2) = P_{(\mu)(\gamma)}(p)\;(p^2 - m^2 + i\epsilon)^{-1}.$$

Inserting this expression into 2.25, we obtain the expression for the free field propagator in momentum space,

$$\Delta^{o}{}_{(\mu)(\gamma)}{}^{ij}(p) = \int_o^\infty dm^2\;\rho^{oij}(m^2)\,P_{(\mu)(\gamma)}(p)\,(p^2 - m^2 + i\epsilon)^{-1} \qquad (2.26)$$

$$= P_{(\mu)(\gamma)}(p)\sum_r \delta_{ir}\delta_{rj}(p^2 - m^2 + i\epsilon)^{-1},$$

where all the spin dependence is contained in the projection operator $P_{(\mu)(\gamma)}(p)$.

The propagator for the interpolating fields $\Psi_{(\mu)}{}^{i}(x)$ developed by Rivers (4) contains terms corresponding to current divergences and traces of the fields, applicable to the general case. For simplicity, we assume that the spin 2 fields of interest here contain no spin 1 or spin 0 components corresponding to these extra terms. The propagator for the interpolating fields $\vec{\Psi}_{(\mu)}(x)$ is defined by

$$\Delta'^{ij}_{(\mu)(\gamma)}(x-y) \equiv -i\langle 0|T\{\Psi^{i}{}_{(\mu)}(x)\;\Psi^{j}{}_{(\gamma)}{}^{\dagger}(y)\}|0\rangle \qquad (2.27)$$

$$= U_{ik}[-i\langle 0|T\{\varphi^{k}{}_{(\mu)}(x)\;\varphi^{l}{}_{(\gamma)}(y)^{\dagger}\}|0\rangle]U^{\dagger}{}_{lj}$$

$$= U_{ik}\,\Delta^{g}{}_{(\mu)(\gamma)}{}^{kl}(x-y)\;U^{\dagger}{}_{lj},$$

which relates the mixed to the unmixed propagators.

Taking the Fourier transform of 2.27, we find the momentum space propagator for the interpolating fields

$$\Delta'_{(\mu)(\gamma)}{}^{ij}(p) = \int_0^\infty dm^2\ \rho^{ij}(m^2)\ P_{(\mu)(\gamma)}(p)\ (p^2 - m^2 + i\epsilon)^{-1}\ , \qquad (2.28)$$

which allows the definition

$$\Delta'_{(\mu)(\gamma)}{}^{ij}(p) \equiv P_{(\mu)(\gamma)}(p)\ \Delta'^{ij}(p), \qquad (2.29)$$

with the last factor on the right hand side defined in 2.10.

From this form it is evident that the spin dependence of the T-matrix can be included in the form factors, as in 2.22. Since we are using the field theory formalism only as a basis for a consistent notation, we shall not deal with the complications arising from the use of high-spin fields. The purpose here is simply to establish a formalism in which unitary symmetry may be exploited in a consistent and systematic manner. The sole object of the foregoing treatment is to demonstrate that the inclusion of spin need not be an essential complication in applying the theory in a phenomenological framework.

III. REPRESENTATION MIXING AND THE TWIN-PEAKED A_2 MASS DISTRIBUTION

A. Introduction

Experimental groups at CERN (5.a), (5.b) and Brookhaven National Laboratory (5.c) have established the existence of a twin-peaked meson mass distribution centered at 1297 MeV in the reaction

$$\pi^- + p \rightarrow X^- \text{ (missing mass)} + p. \qquad (3.1)$$

Decay modes for the "missing mass" meson resonance $X^- \rightarrow \eta+\pi^-$ and $X^- \rightarrow K^-+K^o$ studied by BNL (5.c) indicate that the quantum numbers of X^- are those usually associated with the $A_2(1300)$ meson, which is thought to be the isovector component of a tensor (spin 2) octet. A single Breit-Wigner resonance amplitude gives an extremely poor fit to the twin-peaked mass distribution, indicating the existence of a second A_2-type meson with a mass close to that of the $A_2(1300)$. We assign this new meson to a 27-dimensional irreducible representation of SU(3) and show that the representation mixing formalism gives an excellent fit to not only the twin-peaked mass distribution seen by these experimental groups, but also to some other data in which single-A_2 meson models seem to falter (6), (7).

A model in which the 27-plet arises naturally in conjunction with other known meson multiplets with positive parity is the quark model (8). The simplest configuration of quarks which includes a 27-plet is the s-wave (zero orbital angular momentum) four-quark state $|q\bar{q}q\bar{q}\rangle$, which has the group decomposition

$$3 \times 3 \times \bar{3} \times \bar{3} = 27 + 10 + \overline{10} + 8 + 8 + 8 + 8 + 1 + 1.$$

Since mesons belong to self-conjugate multiplets, the 10 and $\overline{10}$ are neglected. This leaves the usual four octets, labelled by $A_2(2^+)$, $A_1(1^+)$,

$B(1^+)$, and $\pi_v(0^+)$, two singlets, labelled by $f'(2^+)$ and $f''(?^+)$, and the 27-plet, which we shall label by $A_2'(2^+)$. Hence the s-wave, four-quark states provide a basis for all the known positive-parity mesons, plus a few which are not so well known. Since the isovector component of the 27-plet has its other quantum numbers identical to those of the $A_2(2^+)$ isovector, some mixing may be expected to occur between these representations as well as the usual singlet-octet mixing(1). The formalism of the quark model has not been used in the development of our theory; use has been made of the SU(3) Clebsch-Gordan coefficients relating the various coupling constants only. The above is intended to demonstrate a model in which the assignment of the A_2' to a 27-plet is a natural and useful assumption.

B. The T-Matrix for the General Mixing Case

As developed in the previous chapter, mixing of the SU(3) states gives rise to a mass matrix $\underset{\sim}{M}_g^2$, with elements usually considered to correspond to matrix elements of an interaction H_I. The mass matrix has the general form

$$(\underset{\sim}{M}_g^2)_{ij} \equiv D_{ij} - i A_{ij} \tag{3.2}$$

which, to lowest order in H_I, is given by

$$D_{ij} - i A_{ij} = \int dE \, \langle \psi_i | H_I | \psi_j \rangle \, (E - E_o + i\epsilon)^{-1}. \tag{3.3}$$

Invariance under TCP implies that

$$M_{21}^2 \equiv D_{21} - i A_{21} = D_{12}^* - i A_{12}^*. \tag{3.4}$$

This constraint must be satisfied for the mass matrix derived in Chapter II, since TCP invariance must hold for LSZ field theory.

In the previous chapter the mass matrix $\underset{\sim}{M}_g^2$ is defined by the inverse of a unitary transformation of the diagonal mass matrix $\underset{\sim}{M}^2$. Defining the

unitary matrix U by

$$U \equiv u^{-1/2} \begin{pmatrix} a & b \\ c & d \end{pmatrix} , \tag{3.5}$$

$u = ad - bc,$

and choosing u real, we obtain

$$U^{\dagger} = U^{-1} = u^{-1/2} \begin{pmatrix} a^{*} & c^{*} \\ b^{*} & d^{*} \end{pmatrix} = u^{-1/2} \begin{pmatrix} d & -b \\ -c & a \end{pmatrix} ,$$

which gives $a^{*} = d$, $b = -c^{*}$, and

$$U = u^{-1/2} \begin{pmatrix} a & b \\ -b^{*} & a^{*} \end{pmatrix} . \tag{3.6}$$

Then

$$\underset{\sim}{M}_{g}^{2} = U^{-1} \underset{\sim}{M}^{2} U = \frac{1}{u} \begin{pmatrix} aa^{*}m_1^{2} + bb^{*}m_2^{2} & a^{*}b(m_1^{2} - m_2^{2}) \\ ab^{*}(m_1^{2} - m_2^{2}) & bb^{*}m_1^{2} + aa^{*}m_2^{2} \end{pmatrix}, \tag{3.7}$$

where $m_j^{2} \rightarrow m_j^{2} - i m_j \gamma_j$, $j = 1,2$, are the complex masses of the physical states. Hence we can identify

$$M_1^{2} - iM_1 \Gamma_1 = u^{-1}\{aa^{*}m_1^{2} + bb^{*}m_2^{2} - i(aa^{*}m_1\gamma_1 + bb^{*}m_2\gamma_2)\}, \tag{3.8}$$

$$M_2^{2} - iM_2 \Gamma_2 = u^{-1}\{bb^{*}m_1^{2} + aa^{*}m_2^{2} - i(bb^{*}m_1\gamma_1 + aa^{*}m_2\gamma_2)\},$$

$$M_{12}^{2} = D_{12} - iA_{12} = u^{-1}\{a^{*}b(m_1^{2} - m_2^{2}) - i\, a^{*}b(m_1\gamma_1 - m_2\gamma_2)\},$$

$$M_{21}^{2} = D_{12}^{*} - iA_{12}^{*} = u^{-1}\{ab^{*}(m_1^{2} - m_2^{2}) - i\, ab^{*}(m_1\gamma_1 - m_2\gamma_2)\},$$

and the TCP condition 3.4 on the off-diagonal elements is automatically satisfied.

A 2x2 unitary matrix has four free parameters which can be represented

by

$$\beta = \theta + i\varphi, \tag{3.9}$$

$$u^{-1/2}\, a \rightarrow a \cos\beta,$$

$$u^{-1/2}\, b \rightarrow -b \sin\beta,$$

where a and b have been redefined, and

$$U = \begin{pmatrix} a\cos\beta & b\sin\beta \\ -b\sin^{*}\beta & a\cos^{*}\beta \end{pmatrix} .$$

With this parameterization of the U matrix, 3.8 becomes

$$M_1^2 = a^2 |\cos\beta|^2 m_1^2 + b^2 |\sin\beta|^2 m_2^2, \tag{3.10}$$

$$M_2^2 = b^2 |\sin\beta|^2 m_1^2 + a^2 |\cos\beta|^2 m_2^2,$$

$$M_{12}^2 = ab \cos^{*}\beta \sin\beta\, (m_1^2 - m_2^2),$$

$$M_{21}^2 = ab \cos\beta \sin^{*}\beta\, (m_1^2 - m_2^2),$$

where all the masses are considered to be complex, $m_j^2 \rightarrow m_j^2 - i m_j \gamma_j$, etc.

The procedure applied for singlet-octet representation mixing takes $a = b = 1$, $\varphi = 0$, and $\beta = \theta$. This is the scalar mixing case treated by Coleman and Schnitzer (3) and by Rivers (4). In this case we obtain

$$M_1^2 = \cos^2\theta\, m_1^2 + \sin^2\theta\, m_2^2, \tag{3.11}$$

$$M_2^2 = \sin^2\theta\, m_1^2 + \cos^2\theta\, m_2^2,$$

$$M_{12}^2 = M_{21}^2 = \frac{1}{2} \tan 2\theta\, (m_1^2 - m_2^2).$$

In terms of the SU(3) coupling constants, the T-matrix 2.22 can be written in the form

$$T = (F_1, F_2)\ (t\,\underset{\sim}{1} - \underset{\sim}{M}_g^{\,2})^{-1} \begin{pmatrix} G_1 \\ G_2 \end{pmatrix} \tag{3.12}$$

$$= (F_1, F_2) \frac{\begin{pmatrix} t - M_2^{\,2} & \frac{1}{2}\tan 2\theta\,(m_1^{\,2} - m_2^{\,2}) \\ \frac{1}{2}\tan 2\theta\,(m_1^{\,2} - m_2^{\,2}) & t - M_1^{\,2} \end{pmatrix}}{(t - m_1^{\,2})(t - m_2^{\,2})} \begin{pmatrix} G_1 \\ G_2 \end{pmatrix}.$$

The F's and G's are the vertex functions consisting of the products of Clebsch-Gordan coefficients and the appropriate reduced matrix elements describing the production and decay of the states carrying irreducible representations of SU(3).

C. The A_2 Mass Distribution with Scalar Mixing

The reaction investigated here is

$$\pi^- + p \rightarrow X^- + p \tag{3.13}$$
$$\qquad\qquad \hookrightarrow \rho + \pi,\ \eta + \pi,\ K^- + K^o,$$

where X^- may be either the octet isovector denoted by A_2, or the 27-plet isovector denoted by A_2'. We shall assume that the production is predominantly due to ρ and η exchange between the incident pion and the target proton, as depicted in the diagram in Fig. 1. The differential cross section in terms of the total center of mass energy t of the two-particle final state $|x_1 x_2\rangle$ can be written in the form

$$\left.\frac{d\sigma}{dt}\right|_f = K_f\ |T_f|^2\ , \tag{3.14}$$

where K_f is a phase space factor; the dependence of T_f on the remaining variables has been neglected. The T-matrix has the form

$$T_f = \sum_i T_{fi} = (F_f, F'_f)\ (t\,\underset{\sim}{1} - \underset{\sim}{M}_g^{\,2})^{-1} \begin{pmatrix} G \\ G' \end{pmatrix}\ , \tag{3.15}$$

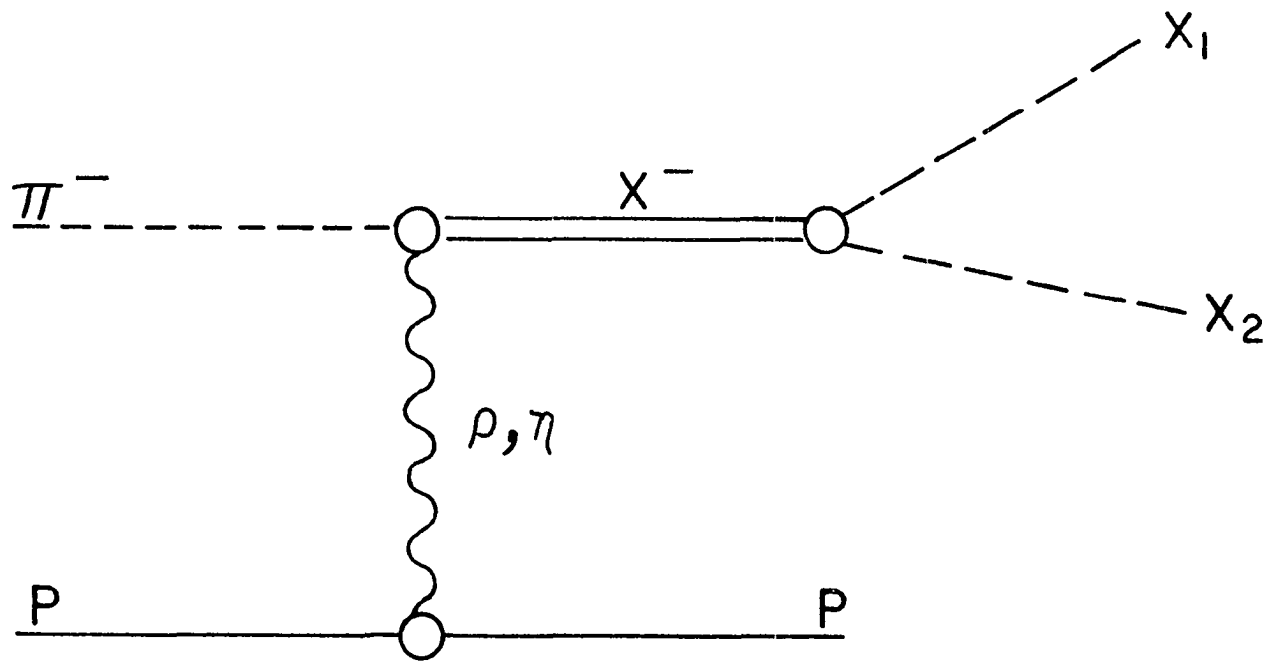

Fig. 1. Exchange Diagram for the Reaction $\pi^- + p \rightarrow X^- + p$

Here X^- is either the octet (A_2) or the 27-plet (A_2'). The final state particles, x_1 and x_2, can be either ρ-π, η-π, or K^--K^o.

where

$$G = \sum_i F_{i\pi A} \frac{\bar{u}(p_f)\, \Gamma_{iNN}\, u(p_i)}{t - m_i^2}, \qquad i = \rho, \eta,$$

and similarly for G'. The F's are the form factors for A_2 production (or decay) into which has been incorporated all the spin-dependent factors from the numerators of the propagators. The helicity and isospin labels have also been suppressed. The missing-mass spectrometer measures essentially the differential cross section for all final decay states. Since the data are in the form of number of events/MeV versus t, and the shape of the mass distribution is apparently independent of the incident pion momentum, the phase space factors have been neglected in obtaining numerical fits to the data.

In order to minimize the number of free parameters, the scalar mixing form has been adopted. This implies that the unitary transformation U relating the mixed states to the unmixed states is given by

$$U = \begin{pmatrix} \cos\theta & \sin\theta \\ -\sin\theta & \cos\theta \end{pmatrix}. \tag{3.16}$$

Both the octet, A_2, and the 27-plet, A_2', have the quantum numbers $I^G(J^P)C = 1^-(2^+)+$. Using the SU(3) Clebsch-Gordan coefficients of McNamee and Chilton (9), we obtain the relations between the various coupling constants. For the octet, the coupling constants of interest here are defined by

$$\langle A_2 | \rho\pi \rangle = \frac{\sqrt{2}}{\sqrt{3}} F_{TVP}, \tag{3.17}$$

$$\langle A_2 | \eta\pi \rangle = \frac{\sqrt{2}}{\sqrt{5}} D_{TVP},$$

$$\langle A_2 | K\bar{K} \rangle = -\frac{\sqrt{3}}{\sqrt{5}} D_{TPP},$$

and $D_{TVP} = F_{TPP} = 0$ by C (or G) invariance. For the 27-plet,

$$\langle A_2' | \eta\pi \rangle = \frac{\sqrt{3}}{\sqrt{5}} D'_{TPP}, \tag{3.18}$$

$$\langle A_2' | K\bar{K} \rangle = \frac{\sqrt{2}}{\sqrt{5}} D'_{TPP},$$

$$\langle A_2' | \rho\pi \rangle = 0,$$

and $D'_{TVP} = 0$ by G invariance. In these definitions, the subscripts T (tensor), V (vector) and P (pseudoscalar) describe the spin and parity of the particle states. In the following these subscripts will be omitted unless they are required for clarity.

Note that $\langle A_2 | K^*\bar{K} \rangle$ vanishes because $M_{K^*\bar{K}} > M_{A_2}$; otherwise it would be proportional to F, which is known to be large. The coupling constants for the mixed states are defined by 2.21,

$$\vec{f}^{\dagger} = \vec{F}^{\dagger} U , \tag{3.19}$$

$$\vec{g} = U^{\dagger} \vec{G} ,$$

where β_g has been replaced by f, β by F, α_g by g, and α by G. The scalar mixing form of the U-matrix inserted into these expressions gives

$$(f_1^K, f_2^K) = (-\frac{\sqrt{3}}{\sqrt{5}} D, \frac{\sqrt{2}}{\sqrt{5}} D') \begin{pmatrix} \cos\theta & \sin\theta \\ -\sin\theta & \cos\theta \end{pmatrix}, \tag{3.20}$$

or

$$f_1^K = -\frac{\sqrt{3}}{\sqrt{5}} D \cos\theta \, (1 + \frac{2}{3} r \tan\theta)$$

$$f_2 = -\frac{\sqrt{3}}{\sqrt{5}} D \cos\theta \, (\tan\theta - \frac{2}{3} r),$$

where $r \equiv \frac{D'}{D}$. Similarly,

$$f_1^{\eta} = \frac{\sqrt{2}}{\sqrt{5}} D \cos\theta \left(1 - \frac{3}{2} r \tan\theta\right), \tag{3.21}$$

$$f_2^{\eta} = \frac{\sqrt{2}}{\sqrt{5}} D \cos\theta \left(\tan\theta + \frac{3}{2} r\right),$$

$$f_1^{\rho} = \frac{\sqrt{2}}{\sqrt{3}} F \cos\theta, \text{ and}$$

$$f_2^{\rho} = \frac{\sqrt{2}}{\sqrt{3}} F \sin\theta.$$

In terms of the physical (mixed) states and their associated coupling constants, the T-matrix becomes

$$T_f = (f_1^f, f_2^f) \begin{Bmatrix} \frac{1}{t - m_1^2} & 0 \\ 0 & \frac{1}{t - m_2^2} \end{Bmatrix} \begin{pmatrix} g_1 \\ g_2 \end{pmatrix}. \tag{3.22}$$

The differential cross sections for the three final states of interest are

$$\left.\frac{d\sigma}{dt}\right)_{K\bar{K}} = K_K \frac{3}{5} \left|D\, g_1 \cos\theta\right|^2 \left| \frac{1 + \frac{2}{3} r \tan\theta}{t - m_1^2} + \frac{(\tan\theta - \frac{2}{3} r)n}{t - m_2^2} \right|^2, \tag{3.23}$$

$$\left.\frac{d\sigma}{dt}\right)_{\eta\pi} = K_\eta \frac{2}{5} \left|D\, g_1 \cos\theta\right|^2 \left| \frac{1 - \frac{3}{2} r \tan\theta}{t - m_1^2} + \frac{(\tan\theta + \frac{3}{2} r)n}{t - m_2^2} \right|^2,$$

$$\left.\frac{d\sigma}{dt}\right)_{\rho\pi} = K_\rho \frac{2}{3} \left|F\, g_1 \cos\theta\right|^2 \left| \frac{1}{t - m_i^2} + \frac{n \tan\theta}{t - m_2^2} \right|^2,$$

where $n \equiv g_2/g_1$.

From the forms of these expressions it is easy to see the structure of the mass distribution for special values of the parameters. If $\frac{D^2}{F^2} \ll 1$, as would be expected from the observed A_2 branching ratio, then the missing-mass cross section is due mainly to the ρ-π decay mode, and the double peak results from the interference between the two poles. The single peak observed in the K^--K^o decay mode by BNL (5c) would result from the condition

$$\tan \theta \approx \frac{2}{3} r = \frac{2}{3} \frac{D'}{D} . \qquad (3.24)$$

This condition allows for a double-peaked distribution for the η-π decay mode, as suggested by the BNL data. With this interpretation, one would expect to find that m_1^2 is the mass of the A_2^H ($m_H = 1311 \pm 5$ MeV, $\Gamma_H = 21 \pm 10$ MeV) and m_2^2 is the mass of the A_2^L ($m_L = 1269 \pm 5$ MeV, $\Gamma_L = 24 \pm 10$ MeV) found by the BNL group.

The important point here is that the absence of a K^--K^o peak for the lower pole does not imply that the A_2^L can not have $J^P = 2^+$. This is a critical point in fitting the data because the rather steep and deep dip in the mass distribution at 1297 MeV requires interference between the two poles, which in turn implies that the two corresponding resonances must have exactly the same quantum numbers, except for their SU(3) representation labels. This is confirmed by the fact that the confidence level (indicating the goodness of the fit) for the case of two non-interfering Breit-Wigner resonance amplitudes is not significantly better than that obtained for a single-pole fit.

Taking 3.24 as an equality, and defining

$\epsilon \equiv \left|\frac{D}{F}\right|^2$, and $K = K_i \left|F\, g_1 \cos\theta\right|^2$ for $i = \rho, \eta, K$, (the small phase space differences for the final states are being neglected), we can write the cross sections in the form

$$\left.\frac{d\sigma}{dt}\right|_{K\bar{K}} = \frac{3}{5}\,\epsilon\, K \left|\frac{1 + \tan^2\theta}{t - m_1^2}\right|^2 , \qquad (3.25)$$

$$\left.\frac{d\sigma}{dt}\right|_{\eta\pi} = \frac{2}{5}\,\epsilon\, K \left|\frac{1 - \frac{3}{2}\tan^2\theta}{t - m_1^2} + \frac{\frac{5}{2}\, n \tan\theta}{t - m_2^2}\right|^2 ,$$

$$\left.\frac{d\sigma}{dt}\right|_{\rho\pi} = \frac{2}{3}\, K \left|\frac{1}{t - m_1^2} + \frac{n \tan\theta}{t - m_2^2}\right|^2 ,$$

$$\left.\frac{d\sigma}{dt}\right|_{MM} = \sum_i \left.\frac{d\sigma}{dt}\right|_i , \text{ for } i = K\bar{K},\ \eta\pi,\ \rho\pi.$$

An estimate of the magnitude of ϵ is obtained by setting

$$\frac{\int \left.\frac{d\sigma}{dt}\right|_{\eta\pi} dt}{\int \left.\frac{d\sigma}{dt}\right|_{\rho\pi} dt} \approx \frac{3}{5}\,\epsilon \approx \frac{\Gamma(A_2 \to \eta\,\pi)}{\Gamma(A_2 \to \rho\,\pi)} \approx \frac{.15}{.80} ,$$

which gives $\epsilon \approx 0.3$.

D. Results of the Data Fitting

As reviewed by Benz, et al. in (5.b), there are three significantly different data sets relevant to the mass distribution associated with the A_2 meson. A brief description of these data sets follows.

1. CERN missing-mass spectrometer data (5.a)

These data consist of a compilation of events seen in the reaction 3.1 at incident pion lab momenta of 6.0 and 7.0 GeV/c. The compilation

of over 4,000 events in 5 MeV bins is characterized by a peak at 1282.5 MeV, a sharp dip at 1297.5 MeV, and a peak at 1312.5 MeV, with the peak heights having a ratio of 108:22:103 above background (in arbitrary units).

2. Compilation of boson spectrometer and missing-mass data (5.b)

The boson spectrometer group at CERN ran the same reaction at incident pion momenta of 2.55, 2.60 and 2.65 GeV/c. The compilation of the two CERN experiments (in 10 MeV bins) is characterized by a peak at 1285 MeV, a sharp dip at 1295 MeV, and a peak at 1315 MeV, with peak height ratios 63:18:72 above background (in arbitrary units). The shapes and peak positions of the mass distributions are similar for all the incident pion momenta. Since the compilation of all the experimental data from both CERN experiments carries an impressive statistical weight, prime importance was attached to the parameters giving the best fit to these data. This is significant only because in this compilation the higher peak is somewhat larger than the lower peak, while the reverse of this situation is seen in data set 1. However, as will be seen, an excellent fit to the compiled data also gives a reasonable fit to the finer-grained data set 1.

3. BNL 80-inch bubble chamber data (5.c)

The outstanding feature of the BNL data is the single peak at 1311 MeV seen for the K^{-}-K^{o} decay mode, while the missing-mass distribution is seen as a double-peaked curve similar to the CERN data. Although the BNL statistics are extremely poor compared to the CERN data, it is felt that the absence of the second peak for the K-K decay mode is a fundamental property of the underlying physics, and any attempt to explain these phenomena should include the possibility of single peaks for certain

reactions as well as double peaks for others. The condition 3.24 automatically provides a good fit to the K^--K^o data since it implies a single peak at the required mass. For this reason numerical fits to the BNL data, while reasonable, were not given any significance. It should also be noted here that the absence of the lower peak for the K-K decay mode led the BNL group to the conclusion that A_2^L should have $J^P = 1^-, 3^-, \ldots$. This conclusion is not only unnecessary, as is evident by the form of the cross section in 3.25, but also provides an unreliable fit to the twin-peaked mass distribution, since in this case there could be no interference between resonances with different spins and parities.

A least-squares fitting procedure utilizing the MINFUN program on the Iowa State University IBM 360/65 was used to obtain a seven parameter fit to the compiled CERN data (set 2). The best fit had $\chi^2 = 5.2$ for 16 data points (Fig. 2) with the following parameters:

$$m_1 = 1309 \text{ MeV}, \qquad \gamma_1 = 33 \text{ MeV}, \tag{3.26}$$

$$m_2 = 1299 \text{ MeV}, \qquad \gamma_2 = 24 \text{ MeV},$$

$$\theta = 0.213\ \pi = 38.6^o,$$

$$n \tan\theta = 0.12 + 0.61\ i.$$

The SU(3) masses and widths, from 3.11, are

$$M_1 = 1301 \text{ MeV}, \qquad \Gamma_1 = 29 \text{ MeV},$$

$$M_2 = 1296 \text{ MeV}, \qquad \Gamma_2 = 27 \text{ MeV}.$$

These same parameters gave $\chi^2 = 30$ for the 40 points of data set 1. Small differences in the parameters were able to reduce this to $\chi^2 = 25$, but, as discussed previously, the fits to set 2 were taken to be the most significant.

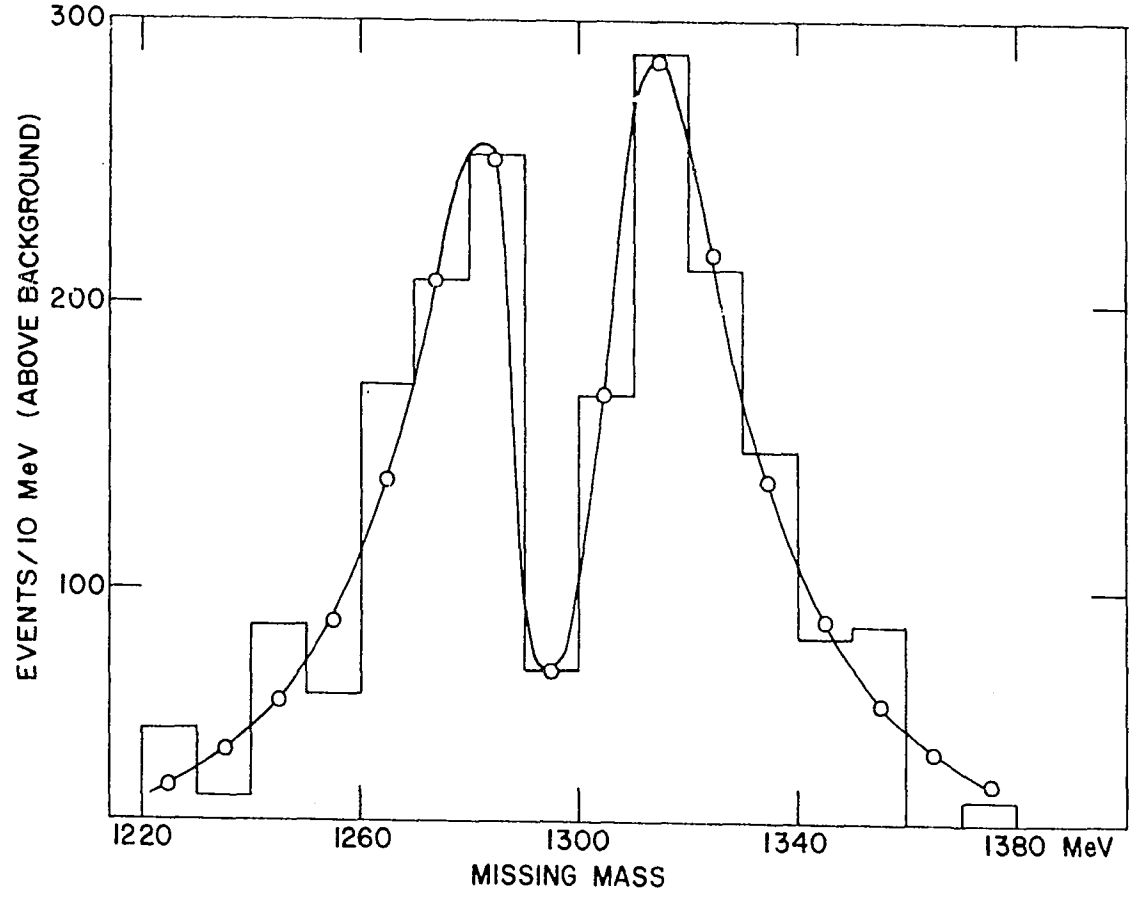

Fig. 2. Fit to the Compiled CERN Missing-Mass and Boson Spectrometer Data

This fit was obtained using the amplitudes which reproduce the single-peaked distribution for the K-K decay mode seen by the BNL group (5.c). The data were taken from Benz, et al. (5.b).

Since ϵ is small, the main part of the missing-mass distribution is due to the ρ-π decay mode, which depends only on the combination $n \tan\theta = (g_2/g_1) \tan\theta$. For this reason the fit does not serve as a critical determination of the mixing angle, and the resulting values of the SU(3) masses and widths are not to be taken too seriously.

To summarize, we think of the total mass distribution to be mainly that of the ρ-π decay mode; the η-π decay mode may also give a double-peaked distribution, while the K-K decay mode gives a single peak centered at the position of the higher mass, serving to increase the height of the high peak with respect to that of the low peak. This situation is reflected in the relative peak heights of the compilation of all the CERN data (set 2). Because of a fortuitous relation between the mixing angle and the coupling constants, 3.24, one of the mixed states has a very small K-K decay mode, which accounts for the single peak seen by BNL for this reaction. The mixing formalism then serves to establish relations between several seemingly independent phenomena while retaining all the successes of previous SU(3) models.

As mentioned by Benz, et al. in (5.b), a double-peaked distribution was observed by Anguilar-Genitez, et al., for the decay of the A_2 into K_1^0-$K^{\pm}$, in which case 3.24 would not hold. By relaxing this requirement, fits were obtained to data set 1 (which has events plotted in 5 MeV bins) having $\chi^2 = 20$ for 33 degrees of freedom. The masses and widths obtained from these fits are:

$$m_1 = 1299 \text{ MeV}, \qquad \gamma_1 = 66 \text{ MeV}, \tag{3.27}$$

$$m_2 = 1299 \text{ MeV}, \qquad \gamma_2 = 13 \text{ MeV}.$$

The mixing angle was $\theta = 0.06\ \pi = 10.8^{\circ}$, which gives for the SU(3) masses and widths

$$M_1 = 1299 \text{ MeV}, \qquad \Gamma_1 = 65 \text{ MeV}, \tag{3.28}$$

$$M_2 = 1299 \text{ MeV}, \qquad \Gamma_2 = 15 \text{ MeV}.$$

In this case, all the parameters were taken to be real, and the finer-grained data set 1 was used because the relative peak heights no longer retain the significance attached to them in the previous case.

These mass and width values are not very different from those expected for a double-pole model (10), in which the dipole-shaped mass distribution follows from a degenerate, non-diagonalizable 2x2 mass matrix. The present investigation does not include this case because we have assumed the mass matrix to be diagonalized by the unitary matrix U, which defines the mixing angle.

Also, these mass and width values are much closer to those expected from previous treatments of the 2^+ octet branching ratios, where the decay widths of the other isospin multiplets in the octet are of the same order as γ_1 in 3.27. The question of which set of mass values should be incorporated into the theory depends on the nature of the mass distribution for the K-K decay mode, and therefore can be resolved only by further experimental determination of the structure of this mode.

It is of interest to know whether twin-peaked distributions for other constituents of the tensor octet should be expected, or whether mixing between the f_1, f_8, and f_{27} (isosinglets) would invalidate the previous successful results achieved in treating f_1-f_8 mixing only. As an indication of what might be expected, we cite the mixing formalism of

Resnikoff and Silbar (11), who derive a mass formula for the positive-parity mesons in an SU(6) framework. Their formalism does indeed provide a non-diagonal mass matrix for the octets and 27-plets; however, the mixing of the Y = I = 0 components (f_1,f_8,f_{27}) gives singlet-octet mixing only, because the matrix elements relating f_1 and f_8 to f_{27} vanish. In this instance, the previous treatments of f_1-f_8 mixing need not be disturbed by the presence of a 27-plet. The mixing of the isovector components would provide a new mixing angle, presumably unrelated to the isosinglet mixing angle.

In the data fitting process it was found that for certain values of the parameters a single broad peak was obtained. Since the shape of the mass distribution depends heavily on the amount of interference between the poles, as well as their absolute and relative positions, the question of whether double-peaked structures may be expected for the other isospin multiplets of the tensor octet can only be decided experimentally. The theory is capable of producing both narrow, twin-peaked structures as well as broad, single-peaked structures.

Some of the other consequences of assuming the existence of a spin 2 27-plet include the possible existence of states with isospin 2. Indications of these have been seen off and on in various experimental studies, but no consistent data have yet been accumulated to firmly establish their status. Some ρ^--π^- peaks have been detected (12), but these failed to appear in later experiments. The same situation applies to some K^+-K^+ enhancements detected (12). These indicate the presence of states with isospin 1, strangeness 2, which must also belong to a 27-plet. The difficulty in detecting these states lies in their extremely narrow decay

widths, as seen from both fits to the A_2 mass distribution, especially in 3.27. Much better data is needed in the energy range 1.0 Gev to 1.6 GeV in order to disentangle the meson structure there.

In the following chapters, the representation mixing theory is applied to high energy scattering reactions in which the A_2 meson is involved in the crossed channel process. The parameters obtained above are used in these reactions and successful fits to the relevant data are obtained.

IV. REGGEIZATION OF THE MIXED AMPLITUDES

A. Introduction

The usual prescription for applying Regge theory (13) to high energy scattering is based on the assumption that the partial-wave amplitudes, $T_j(t)$, are meromorphic functions of j in the complex j-plane (neglecting here the possibility of branch points). In the case of spinless particles, the functions T_j are defined by

$$T(s,t) = \sum_j (2j+1)\, T_j(t)\, P_j(\cos\theta), \tag{4.1}$$

which, when inverted, gives

$$T_j(t) = \frac{1}{2}\int_{-1}^{1} (2j+1)\, T(s,t)\, P_j(z) \tag{4.2}$$

$$= \vec{F}_j^{\dagger} \cdot (t\, \underset{\sim}{1} - \underset{\sim}{M}_g^2)^{-1} \cdot \vec{G}_j,$$

where $z = \cos\theta$, and the partial-wave form of the T-matrix element in 2.22 has been used. For the case of a single pole, the prescription amounts to making the correspondence

$$\frac{F_i\, G_i}{t - m^2(j)} \rightarrow \frac{F'_i\, G'_i}{j - \alpha(t)}, \tag{4.3}$$

where Re $M^2(j = j_o) = m_o^2$, the physical mass, and Re $\alpha(t = m_o^2) = j_o$, the physical spin of the particle state appearing in the propagator. If linear Regge trajectories are assumed, $\alpha(t)$ can be written in the form

$$\alpha(t) = j_o + \alpha'(t - m_o^2) + i\,\alpha_{im}(t) \tag{4.4}$$

$$= j_o + \alpha'\{t - (m_o^2 - i\,\alpha_{im}(t)/\alpha')\},$$

and the relation between the decay width, γ_o, and the imaginary part of the trajectory function, α_{im}, is

$$m_o\gamma_o = \alpha_{im}/\alpha'.$$

The pole on the second (unphysical) Riemann sheet of the complex t-plane corresponds to a moving Regge pole in the complex j-plane.

Suppose we make an analogous correspondence for the matrix propagator by taking

$$T_j(t) = \vec{F}'_j \cdot (j \underset{\sim}{1} - \underset{\sim}{A}(t))^{-1} \cdot \vec{G}'_j, \tag{4.5}$$

where

$$(j \underset{\sim}{1} - \underset{\sim}{A}(t)) \equiv \begin{pmatrix} j - \alpha_1(t) & -V_{12} \\ -V_{21} & j - \alpha_2(t) \end{pmatrix},$$

and

$$(j \underset{\sim}{1} - \underset{\sim}{A}(t))^{-1} = \frac{\begin{pmatrix} j - \alpha_2(t) & V_{12} \\ V_{21} & j - \alpha_1(t) \end{pmatrix}}{[j - \alpha_+(t)][j - \alpha_-(t)]},$$

with

$$\alpha_{\pm}(t) = \frac{1}{2}\{\alpha_1 + \alpha_2 \pm [(\alpha_1 - \alpha_2)^2 + 4V_{12}V_{21}]^{1/2}\}$$

defining the eigenvalues of the "spin" matrix $\underset{\sim}{A}(t)$. The new trajectories, $\alpha_{\pm}(t)$, apparently have a branch point where the quantity inside the square brackets vanishes. This complication can be avoided in some special cases. For example, the case $M_1^2 = M_2^2 = M^2$ and $\frac{d}{dt}[(\alpha_1 - \alpha_2)^2 + 4V_{12}V_{21}]\big|_{t=M^2} = 0$ corresponds to having unmixed trajectories whose real parts cross at $t = M^2$. In this case, the mixed trajectories also cross there, which implies that the eigenvalues of the mass matrix are degenerate. The case of a non-diagonalizable mass matrix corresponding to this situation has been treated previously (6), (10), and is not included in the present formalism.

The most straightforward procedure for the Reggeization of the mixing formalism is to apply the usual correspondence to the amplitudes written

in terms of the physical (mixed) states. The t-channel amplitude then has the form

$$T_j^{fi}(t) = \frac{F_1^{\,f}\, G_1^{\,i}}{j - \alpha_1(t)} + \frac{F_2^{\,f}\, G_2^{\,i}}{j - \alpha_2(t)} , \qquad (4.6)$$

where $\mathrm{Re}\ \alpha_1(m_1^2) = \mathrm{Re}\ \alpha_2(m_2^2) = 2$, and $F_k^{\,f}$ is the probability for the physical state k to decay into the final state f, and $G_k^{\,i}$ is the probability for the production of the state k from the initial state i.

Applying the Sommerfeld-Watson transform (13) with the usual assumptions of the analytic structure of the amplitudes, we obtain the Regge form of the scattering amplitude

$$T(s,t) = \sum_i (2\alpha_i+1)\ b_i(t)\ \epsilon_i\ P_{\alpha_i}(-z) + \text{Background integral}, \qquad (4.7)$$

where $b_i(t)$ is the residue of $T_j(t)$ at the pole $j = \alpha_i(t)$, z is the cosine of the scattering angle in the t-channel center of mass system, and the background integral is assumed to be negligible compared to the contributions from the Regge poles at high energies. The signature function ϵ_i is defined by

$$\epsilon_i = \frac{1 \pm e^{-i\pi\alpha_i(t)}}{\sin \pi\, \alpha_i(t)} , \qquad (4.8)$$

where the $\pm$ is determined by the spin of the particle lying on the Regge trajectory through the relation $(-1)^j$ = signature of spin j particle.

B. Reggeization of the Eta Pion-Production Amplitudes

In a treatment of the s-channel reaction

$$\pi^- + p \rightarrow \eta + n, \qquad (4.9)$$

the complications due to the spin of the nucleons must be included in deriving the t-channel amplitudes which are to be Reggeized. For this

purpose we need the kinematic singularity-free, parity conserving helicity amplitudes (KSFPCHA) which are derived in Appendix A. These are the amplitudes which can be cast into the standard form developed by Gell-Mann, et al. (14), and by Wang (15). In the following we sketch briefly the derivation of the Regge amplitudes using some of the notation of the above references.

The helicity amplitudes (16), $f_{cd;ab}$, are defined by

$$\langle q_f,c;p_f,d|S-1|q_i,a;p_i,b\rangle = i(2\pi)^2\delta^4(p_f+q_f-p_i-q_i)\,\frac{2}{M}\,f_{cd;ab}. \qquad (4.10)$$

Taking the scattering plane such that the azimuthal angle $\varphi = 0$, we define the partial wave helicity amplitudes $f^j{}_{cd;ab}(t)$ by the expansion

$$f_{cd;ab}(s,t) = \sum_{j=m}^{\infty} (2j+1)\, f^j{}_{cd;ab}(t)\, d^j{}_{\beta\alpha}(\theta), \qquad (4.11)$$

where $\alpha = a-b$, $\beta = c-d$, $m = \max(|\alpha|,|\beta|)$, and the $d^j{}_{\beta\alpha}(\theta)$ are the rotation matrices when the azimuthal angle is zero. The summation is extended over all the integers by means of the E^j functions defined by Gell-Mann, et al. (14), thus eliminating the problems encountered at negative integral j in the process of analytically continuing the partial wave helicity amplitudes to the complex j-plane. In terms of the KSFPCHA of Wang (15), the expansion 4.11 becomes

$$f^{\pm}_{cd;ab}(s,t) = \sum_{-\infty}^{\infty} (2j+1)\,\{\bar{f}^{\,j\pm}_{cd;ab}(t)\, E^{j+}{}_{\beta\alpha}(\theta) + \bar{f}^{\,j\mp}_{cd;ab}(t)\, E^{j-}{}_{\beta\alpha}(\theta)\}, \qquad (4.12)$$

where

$$f^{\pm}_{cd;ab}(s,t) \equiv \bar{f}_{cd;ab}(s,t) \pm \eta_c\,\eta_d(-1)^{s_c+s_d}(-1)^{\alpha-\beta}\,\bar{f}_{-c\,-d;ab}(s,t),$$

$$\bar{f}_{cd;ab}(s,t) \equiv \left(\sqrt{2}\cos\frac{\theta}{2}\right)^{|\alpha+\beta|}\left(\sqrt{2}\sin\frac{\theta}{2}\right)^{|\alpha-\beta|} f_{cd;ab}(s,t),$$

η_i is the intrinsic parity and s_i is the spin of particle i. The definition implies that Regge trajectories of signature $(-1)^{s_i} = \pm 1$ contribute only to the amplitude $f^{\pm}$ when parity is conserved. A somewhat abbreviated derivation of these formulas is given in Appendix B.

For eta pion-production, reaction 4.9, only the f^+ are nonzero (see Appendix A), and after performing the Sommerfeld-Watson transform on 4.12, neglecting the integrals over the infinite contour in favor of the Regge pole terms, the amplitudes are given by a sum over the positive signature, natural parity Regge poles,

$$f_{cd,ab}(s,t) = \sum_i \left(\sqrt{2}\cos\frac{\theta}{2}\right)^{|\alpha+\beta|}\left(\sqrt{2}\sin\frac{\theta}{2}\right)^{|\alpha-\beta|}(2\alpha_i+1)\epsilon_i\beta^i{}_{cd;ab}E^{\alpha}{}_{i\beta\alpha}(-z),$$

Here the signature factor, ϵ_i, for the A_2 and A_2' trajectories is defined by

$$\epsilon_i \equiv (1 + e^{-i\pi\alpha_i(t)})/\sin\pi\alpha_i(t) \qquad (4.13)$$

and the (now redundant) superscripts $\pm$ have been suppressed.

It is shown by Wang (15) that all the kinematic singularities in the variable s (the total energy in the s-channel center of mass) are contained in the half-angle factors explicitly exhibited. The kinematic singularities in the variable t (the total energy in the t-channel center of mass) for the amplitudes of interest here are derived in Appendix A. In terms of these helicity amplitudes the expression for the s-channel differential cross section in terms of t-channel Regge poles is

$$\frac{d\sigma}{dt} = \frac{1}{4\pi s}\, p_i^{-2}\,(2s_a+1)^{-1}(2s_b+1)^{-1}\sum_{abcd}|f^t{}_{cd;ab}(s,t)|^2 \qquad (4.14)$$

$$= \frac{1}{4\pi s}\, p_i^{-2}\,\frac{1}{2}\,2\,\{|f^t{}_{00;++}(s,t)|^2 + |f^t{}_{00;-+}(s,t)|^2\},$$

where

$$f^{t}_{00;++}(s,t) = \sum_i (2\alpha_i+1)\ \epsilon_i\ \beta^{\alpha}{}_{i\,++}(t)\ E^{\alpha_i+}_{00}(\cos\theta_t), \tag{4.15}$$

$$f^{t}_{00;-+}(s,t) = \sum_i (2\alpha_i+1)\ \epsilon_i\ \beta^{\alpha}{}_{i\,-+}(t)\ E^{\alpha_i+}_{01}(\cos\theta_t),$$

and $\beta^{\alpha}{}_{i\,\underline{+}+}(t)$ is the residue of $f^{j}_{00;\underline{+}+}(t)$ at the pole $j = \alpha_i(t)$. In order to determine the kinematic singularity structure of the residue functions in $\alpha_i(t)$, the asymptotic forms of the E functions are required. These are given by (15)

$$E^{\alpha+}_{00}(\cos\theta_t) \underset{s\to\infty}{\to} \frac{\Gamma(\alpha+\frac{1}{2})}{\sqrt{\pi}\ \Gamma(\alpha+1)} \quad \frac{(s-u)^{\alpha}}{(4p^t\ p^{t\prime})^{\alpha}}\ , \tag{4.16}$$

$$E^{\alpha+}_{01}(\cos\theta_t) \underset{s\to\infty}{\to} \frac{2\alpha^{1/2}}{(\alpha+1)^{1/2}} \quad \frac{\Gamma(\alpha+\frac{1}{2})}{\sqrt{\pi}\ \Gamma(\alpha+1)} \quad \frac{(s-u)^{\alpha-1}}{(4p^t\ p^{t\prime})^{\alpha-1}}\ .$$

The function

$$\frac{\alpha}{\Gamma(\alpha+1)\ \sin\pi\alpha} = \frac{1}{\pi}\quad \Gamma(1-\alpha)$$

is finite for all $\alpha(t)$ continued to the physical s-channel region of the complex j-plane because Re $\alpha \leq 1$ when $t \leq 0$ for all Regge trajectories. The equality holds only for the Pomeranchuk trajectory, which is not involved in this reaction and may not be a Regge trajectory at all. Since the scattering amplitude is assumed to have only Regge poles (we are neglecting the possibility of cuts), the fixed singularities inherent in the E-functions must be canceled by the appropriate factors in the residue functions. Consulting Appendix A for the kinematic t-singularities, and Appendix B for the α-singularities, we find

$$\beta^{\alpha_i}{}_{++} = \frac{1}{2}\,\pi^{-3/2}(t-4M^2)^{-1/2}\Gamma^{-1}(\alpha_i+\tfrac{3}{2})\ \left(\frac{4p^t p^{t\prime}}{4ME_o}\right)^{\alpha_i}\ \alpha_i(\alpha_i+1)\ \gamma^i{}_{++}\ , \qquad (4.17)$$

$$\beta^{\alpha_i}{}_{-+} = \frac{1}{2}\,\pi^{-3/2}(t-4M^2)^{-1/2}\ \Phi^{1/2}\ \Gamma^{-1}(\alpha_i+\tfrac{3}{2})\ \left(\frac{4p^t p^{t\prime}}{4mE_o}\right)^{\alpha_i-1}\ \gamma^i{}_{-+}\ .$$

The factor $\alpha_i(\alpha_i+1)$ in $\beta^{\alpha_i}{}_{++}$ is the Gell-Mann ghost-killing mechmanism discussed in Appendix B. The γ^i's are the reduced residue functions, which we take to be constants, and E_o is a parameter included in order to obtain the proper dimensions. The other factors involving α_i are included simply to remove the α-singularities of the E functions.

These expressions inserted into the expressions for the helicity amplitudes, 4.15 and 4.16, give

$$f_{00;++} = \sum_i (t-4M^2)^{-1/2}\ \Gamma(1-\alpha_i)\,(1+e^{-i\pi\alpha_i})\,(\alpha_i+1)\left(\frac{s-u}{4MEo}\right)^{\alpha_i}\ \gamma^i{}_{++}\ , \qquad (4.18)$$

$$f_{00;-+} = \sum_i (t-4M^2)^{-1/2}\ \Phi^{1/2}\ \Gamma(1-\alpha_i)\,(1+e^{-i\pi\alpha_i})\left(\frac{s-u}{4ME_o}\right)^{\alpha_i-1}\ \gamma^i{}_{-+}\ ,$$

and the expression for the cross section, 4.14, becomes

$$\frac{d\sigma}{dt} = \frac{1}{4\pi s p_s^{\,2}}\left|\frac{1}{t-4M^2}\right|\Bigg\{\left|\sum_i (1+e^{-i\pi\alpha_i})\Gamma(1-\alpha_i)\,(\alpha_i+1)\ \gamma^i{}_{++}\left(\frac{s-u}{4ME_o}\right)^{\alpha_i}\right|^2$$

$$+\Phi\left|\sum_i (1+e^{-i\pi\alpha_i})\Gamma(1-\alpha_i)\ \gamma^i{}_{-+}\ \left(\frac{s-u}{4ME_o}\right)^{\alpha_i-1}\right|^2\Bigg\}, \qquad (4.19)$$

where $\Phi = 4t(p^t p^{t\prime}\sin\theta_t)^2$, p^t ($p^{t\prime}$) is the initial (final) center of mass momentum in the t-channel, and p_s is the initial center of mass momentum in the s-channel. This is the form used in fitting the differential cross section data, as discussed in the next section.

C. Results of the Data Fitting

In fitting the data for the differential cross section for the

reaction 4.9 (17.a) a least-squares method utilizing the MINFUN program on the Iowa State University IBM 360/65 was used. The parameters in the expression 4.19 were chosen as follows:

$$A = \gamma^1_{++} / \gamma^2_{++} , \tag{4.20}$$

$$B = \gamma^1_{-+} / \gamma^2_{++} ,$$

$$C = \gamma^2_{-+} / \gamma^2_{++} ,$$

$$Y = E_o^{-1} .$$

The over all normalization, $N = \gamma^2_{++}$, was chosen by setting

$$\chi^2 = \sum_{E_i t_i} \sum \{[d\sigma(E_i)/dt_i]_{exp} - N^2[d\sigma(E_i)/dt_i]_{calc}\}^2 / (err)^2 ,$$

where err is the experimental error, and requiring

$$\partial\chi^2/\partial N^2 = 0.$$

This leads to the expression

$$N^2 = \sum_{E_i t_i} \sum \{d\sigma(E_i)/dt_i\}_{exp} \{d\sigma(E_i)/dt_i\}_{calc} / (err)^2$$

$$\div \sum_{E_i t_i} \sum \{d\sigma(E_i)/dt_i\}^2_{calc} / (err)^2 .$$

The MINFUN program minimizes the function χ^2 by adjusting the parameters A,B,C, and Y, and N^2 is calculated in terms of these.

The trajectory functions $\alpha_i(t)$ were chosen to satisfy the exchange degeneracy hypothesis and the pion conspirator hypothesis discussed in a previous paper (6) and mentioned in more detail in the next section. The amplitudes used here are somewhat simpler than those in (6) in that one less parameter is required and the t-dependence of the residue functions is more easily interpreted. Although the fits to the differential cross

sections are about the same, a much better fit to the total cross sections for the lower energies was obtained using the above parameterization. This is an important feature of the present work, and is discussed in greater detail in Chapter V.

The fits to the differential cross sections shown in Fig. 3 were obtained for the following parameters:

$A = 0.10$, $B = 1.2$, $C = 4.26$, $Y = 2.4$, and $N = 62.5$.

These parameters give $\chi^2 = 15.2$ for the 30 data points shown in Fig. 3; this represents a confidence level of $\sim$ 90%.

The polarization obtained from these parameters is on the order of 1% at $t = -0.2$ $(GeV/c)^2$, which is consistent with the data (17.b) for $p_{lab} > 5$ GeV/c ($P = -4 \pm 15\%$ at 5 GeV/c, and $P = 2 \pm 7\%$ at 11.2 GeV/c). The sizable polarization at lower energies ($P = 40 \pm 15\%$ at 3.2 GeV/c and $P = 27 \pm 14\%$ at 3.47 GeV/c) is not expected to be reproduced in this calculation because the Regge amplitudes extrapolated to the low energy region should represent only the averaged amplitudes there, with the dip-bump structure from the direct channel resonances averaged out. The Regge amplitudes represent the asymptotic form of the scattering amplitude and can not be expected to contain the full structure of the amplitude in the low energy region.

As is evident in Figs. 4 and 5, the Regge fit to the total cross section (17.c) is excellent in the high energy region, and reproduces an average of the structure seen in the low energy regions. This result is important in the analysis carried out in Chapter V.

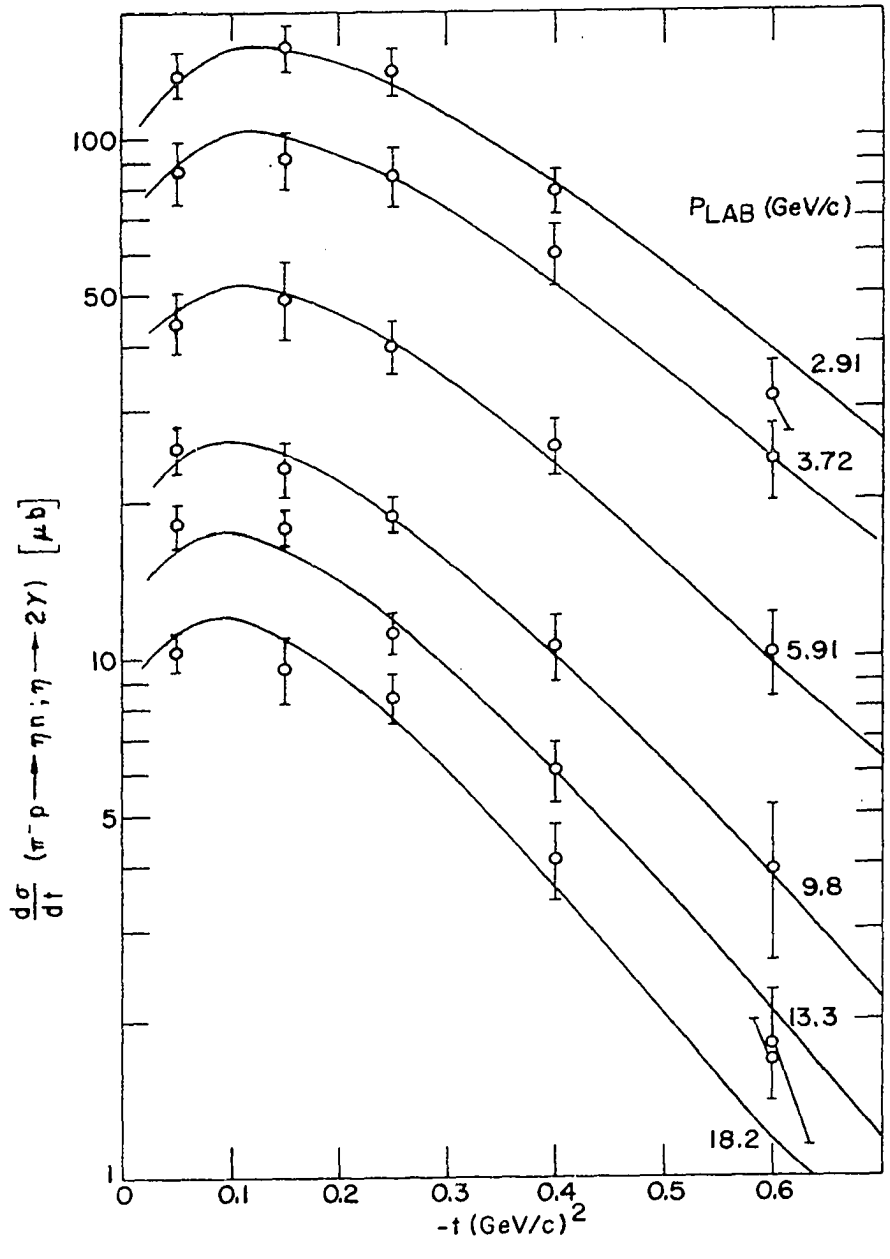

Fig. 3. Regge Fit to the Differential Cross Section Data from (17.a)

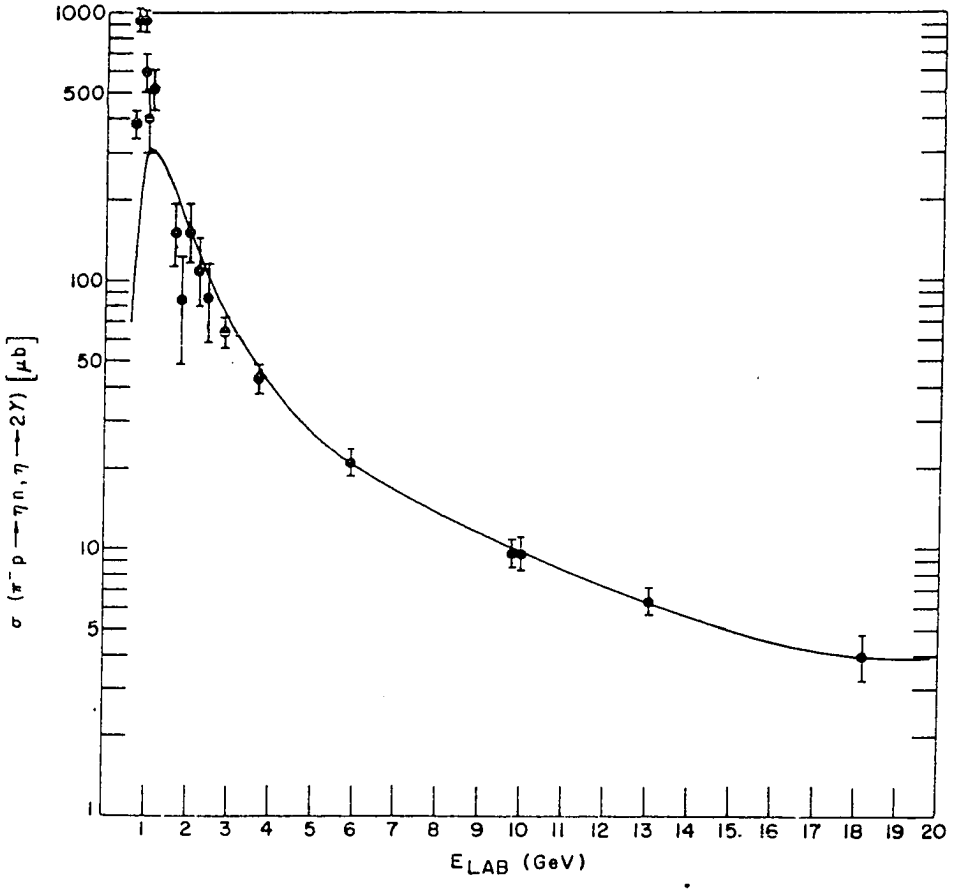

Fig. 4. Regge Fit to the Total Cross Section Data from (17.a) and (17.c)

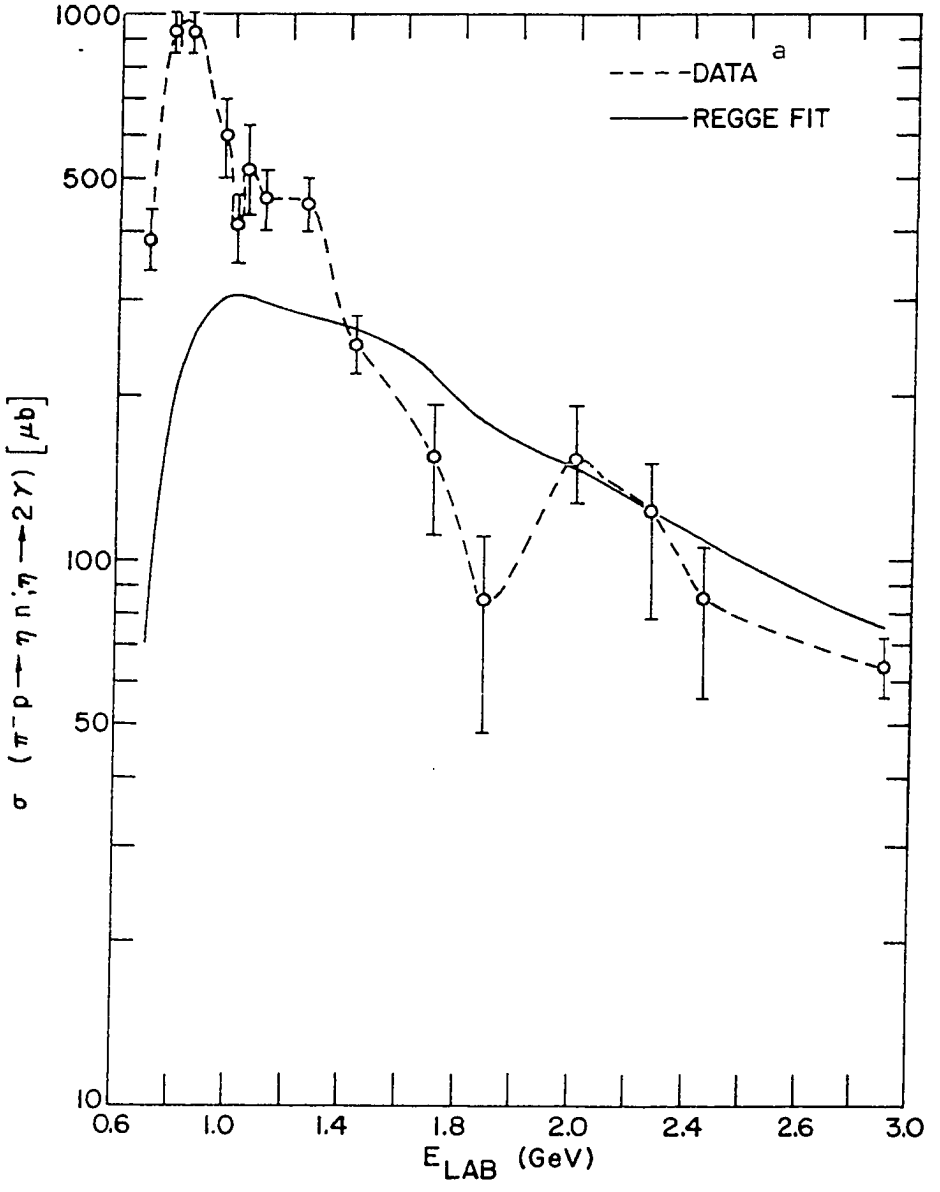

Fig. 5. Regge Fit to the Total Cross Section Data from (17.c) Showing the Resonance Region in Detail

[a] The dashed line is the author's free-hand sketch connecting the data points and is of no further significance.

D. Application to Charged Pion Photoproduction

The well established large forward peak seen by several experimental groups presents another difficulty for the simple Regge model. The difficulty can be best expressed by studying the properties of the invariant amplitudes for the process $\gamma+p \rightarrow \pi^+ + n$. These amplitudes, which are supposed to be free of kinematic singularities, can be written in the form (18)

$$A_1 = t\, F^+_1 + F^+_3 \,, \qquad (4.21)$$

$$A_2 = F^+_1 + \frac{1}{t}(F^-_2 + 2M^2 F^+_3) \,,$$

$\ldots,$

where F^+ is dominated by natural parity ($P = (-1)^J$) trajectories, such as the rho and A_2, and F^- is dominated by unnatural parity ($P = (-1)^{J+1}$) trajectories, such as the π and B. At $t = 0$, these invariant amplitudes must be finite; this requires either "evasion,"

$$F^-_2 = t\, F^-_2{}' \,,$$

$$F^+_3 = t\, F^+_3{}' \,,$$

where the F' are finite at $t = 0$, or "conspiracy,"

$$F^-_2(t = 0) + 2M^2\, F^+_3(t = 0) = 0,$$

in which case neither of the amplitudes is required to vanish at $t = 0$. Either of these two cases leaves the other invariant amplitudes, A_3 and A_4, finite and nothing more need be said about these. In the second case, one must assume that there exists a natural parity trajectory which "conspires" with the pion trajectory at $t = 0$ in order to make the invariant amplitude A_2 finite there. Since the energy dependence of the amplitudes is s^α,

this implies that $\alpha_c(0) = \alpha_\pi(0)$, i.e., that the trajectory of the conspirator must be degenerate with that of the pion at t = 0. The full scattering amplitude in the forward direction ($\cos\theta = 1$, $t \approx 0$) is given entirely by the invariant amplitude A_1, since the other amplitudes are multiplied by a factor of $\sin\theta$ in the expression for the cross section. For this reason, evasion implies a dip in the cross section near t = 0, an implication not supported by the data. Conspiracy, on the other hand, allows for a forward peak due solely to the trajectory which must conspire with the pion in the amplitude A_2. This new trajectory must have the same internal quantum numbers as the $A_2(1300)$ meson, while its trajectory must coincide with the pion trajectory at t = 0.

There is much evidence implying that the $A_2(1300)$ trajectory intercept at t = 0 should be nearly degenerate with the rho trajectory, which has $\alpha(0) = 0.5 - 0.6$. This supports the exchange degeneracy hypothesis (19) which has been successful in reproducing much of the relevant data. The exchange degeneracy hypothesis allows a single trajectory to be drawn through the positions of five observed meson resonances, including the rho, A_2, R, S, T, and perhaps the U (19). A similar trajectory can be drawn through the π, B, R_3 and a few more points where high-mass, high-spin resonances have been indicated by the data. This hypothesis is very useful in eliminating parameters from the theory, and has received much support from theorists.

Also, in fitting the differential cross section for reaction 4.9 with a formalism somewhat similar to that developed in the preceding sections, Austin, et al. (6), found that the trajectory functions

emerging from the fitting process came very close to satisfying the exchange degeneracy and pion conspiracy requirements, viz.

$$\alpha_{A_2}(t) = 0.576 + 0.83\ t, \qquad (4.22)$$

$$\alpha_{A_2'}(t) = -0.02 + 1.19\ t,$$

where $\alpha_{A_2}(t) = \alpha_{rho}(t)$ found in π-N charge exchange and elastic scattering, and $\alpha_{A_2'}(t = 0) = \alpha_{\pi}(t = 0)$. These trajectories were used in the fit described in the last section. As is noted there, the fit to the data is convincing.

In a series of papers by a theoretical group at Trieste (7), the trajectory parameters for the A_2 and pion conspirator are obtained by applying continuous-moment sum rules to charged pion photoproduction. In this method, the low energy data is used as input to a sum rule in order to predict the Regge parameters required to fit the high energy data. The results reported by this group have trajectories very similar to those in 4.22, with small differences probably due to experimental errors incorporated into the data. From these results we draw the conclusion that the formalism developed here for the twin-peaked A_2 mass distribution and applied to eta pion-production is also capable of reproducing the pion photoproduction data.

V. DOLEN-HORN-SCHMID DUALITY IN ETA PION-PRODUCTION

A. Introduction

In a recent series of papers, Dolen, Horn and Schmid (20) present evidence that the resonance structure seen in low energy, direct channel reactions, such as π-N elastic and charge exchange scattering, is in some way generated by Regge trajectory exchange in the crossed channel. They show that the Regge amplitudes which fit the high energy ($E_{lab} \geq 3$ GeV) cross sections can be extrapolated to give an "averaged" fit to the highly structured low energy cross sections. The Regge amplitudes represent asymptotic expressions for the scattering amplitudes and therefore can not be expected to explicitly contain the dip-bump structure produced by the direct channel resonances in the low energy region. This resonance structure, usually attributed to poles on the second Riemann sheet of the s-plane in the scattering amplitudes, must be due to the background integral which is neglected in the region asymptotic in energy, where it is assumed to be dominated by the Regge pole terms.

This theory is applied by partial wave analyzing the extrapolated Regge amplitudes (rather, the proper linear combinations of these amplitudes which correspond to amplitudes of definite total angular momentum and parity, as described for a particular case in Appendix A), and plotting Argand diagrams for these amplitudes (see Appendix C). Analyses of π-N elastic scattering (20), (21) have shown that the Regge amplitudes do indeed generate circles in the Argand diagrams, some of which correspond closely to those seen in a partial wave phase shift analysis of low energy cross section data (22).

The duality between crossed channel Regge poles and direct channel

resonances becomes a "bootstrap" mechanism in reactions having the same quantum numbers for both channels, such as π-π elastic and $\pi+\pi \rightarrow \pi+\omega$ scattering. This bootstrap idea has been applied to several reactions involving the ρ meson (23). It was found that by including daughter trajectories (i. e., trajectories parallel to the ρ trajectory and satisfying the condition $\alpha_d(t=0) = \alpha_\rho(t=0) - \Delta j$, $\Delta j = 2, 4, \ldots$) self-consistency could be obtained between the low energy resonance structure and the high energy Regge structure to a relatively high degree of accuracy.

An alternative interpretation (21) of the duality hypothesis is that some of the Argand circles seen in the analysis of the low energy data may correspond to genuine resonances, while others may simply be a reflection of the fact that the high energy behavior of cross sections, as determined by the Regge form of the amplitude, generates Argand circles just as resonance poles on an unphysical sheet of the complex s-plane do. If all these circles do not correspond to actual resonances, the interpretation of phase shift analyses of the low energy data can not be considered very reliable, since this is the criterion used to determine the resonance structure (22). It is a simple matter to show that the Regge form of the scattering amplitude produces, when partial wave analyzed, an expression which generates families of maxima and minima in the circular Argand diagrams (24). This situation is taken as an indication that the Dolen-Horn-Schmid duality hypothesis can not be a correct interpretation of the Argand diagrams because these families of resonances do not seem to show up experimentally. A counter-argument to this interpretation is that perhaps these resonance families do exist, but their weak coupling to other states renders their detection difficult.

In any case, an analysis of an inelastic reaction involving the same isospin 1/2 resonances seen in the elastic π-N reaction is of interest. The Regge analysis of eta pion-production discussed in Chapter IV provides a suitable example which can be directly compared with the π-N elastic and charge exchange analysis (21). As is evident in Figs. 4 and 5, our amplitudes do provide an averaged fit to the low energy cross section down to E_{lab} = 1 GeV ($W = \sqrt{s}$ = 1.67 GeV) and should be able to reproduce the resonance structure above that energy reasonably well.

B. Interpretation of the Argand Diagrams

The relation between the amplitudes of definite total angular momentum and parity and the t-channel Reggeized helicity amplitudes is derived in Appendix A. The Argand diagrams produced from the amplitudes have the general appearance expected from the analysis of an inelastic S-matrix element carried out in Appendix C. A sample of the results (the diagram for $j = \frac{9}{2}$) is shown in Fig. 6. In order to avoid the complications arising from a possible additional phase shift corresponding to the non-resonant background the maxima and minima of the absolute values of the amplitudes were taken to indicate the positions of resonances, as suggested by Lovelace (22). With this criterion, a highly absorptive resonance would be seen as a sharp dip in the elastic channel inelasticity parameter r, and an elastic resonance would be seen as a maximum in r as $r \to 1$. In the inelastic amplitude, Equation 6.72 of Appendix C, the magnitude of the scattering amplitude $T_{\ell\pm}$ is given by

$$|T_{\ell\pm}| = \{(1 - r)(1 + s)\}^{1/2}, \tag{5.1}$$

where s is the inelasticity parameter for eta-nucleon elastic scattering.

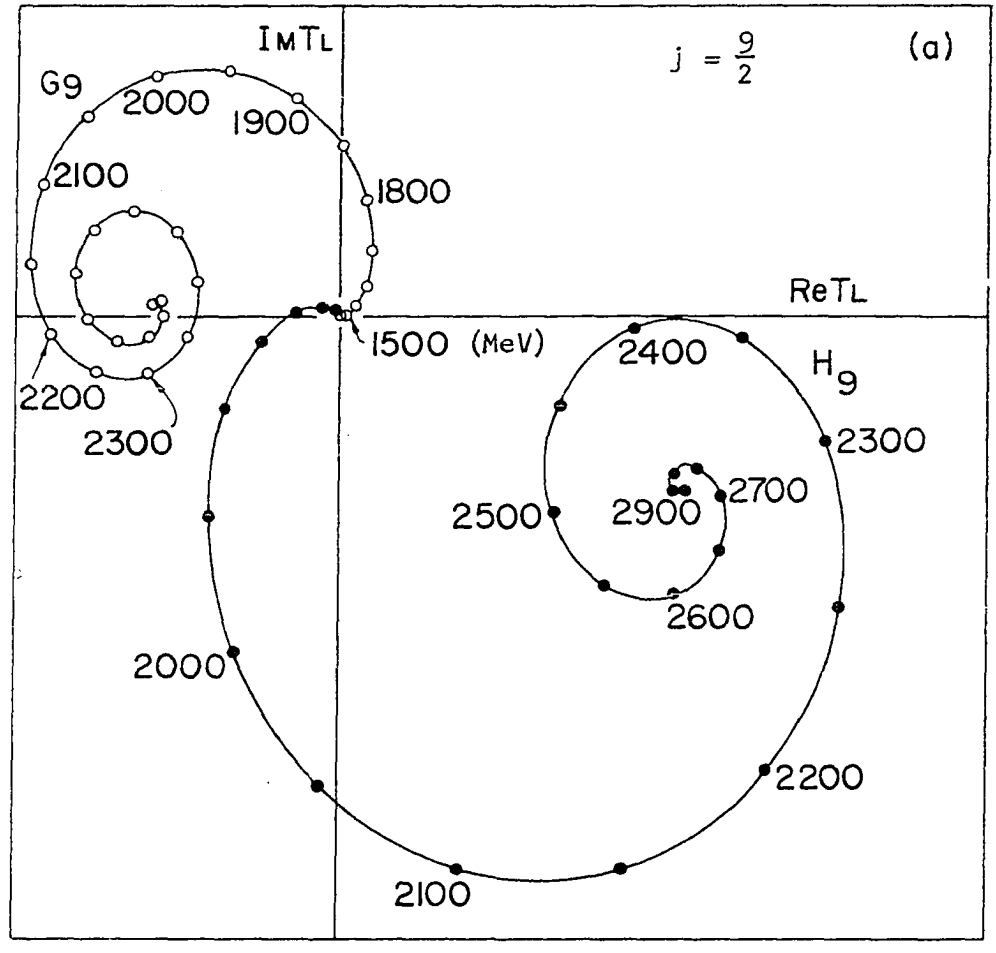

Fig. 6.a. Argand Diagrams for $J = \frac{9}{2}$ Amplitudes

Fig. 6.b. Absolute Value of the Partial Wave Amplitude for $J = \frac{9}{2}$

Fig. 6.c. Phase Shift of the Partial Wave Amplitude for $J = \frac{9}{2}$ Measured from the Real T_L Axis

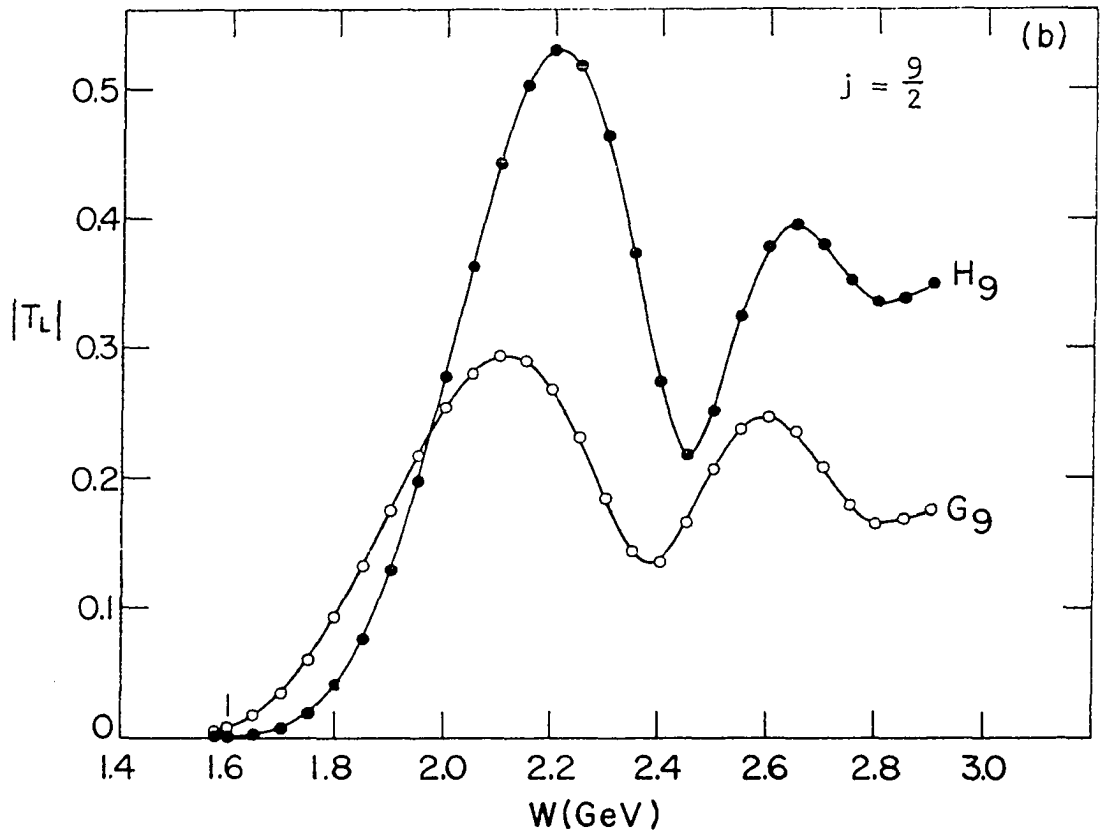
(b)
j = 9/2
H9
G9
|TL|
0.5
0.4
0.3
0.2
0.1
0
1.4
1.6
1.8
2.0
2.2
2.4
2.6
2.8
3.0
W(GeV)

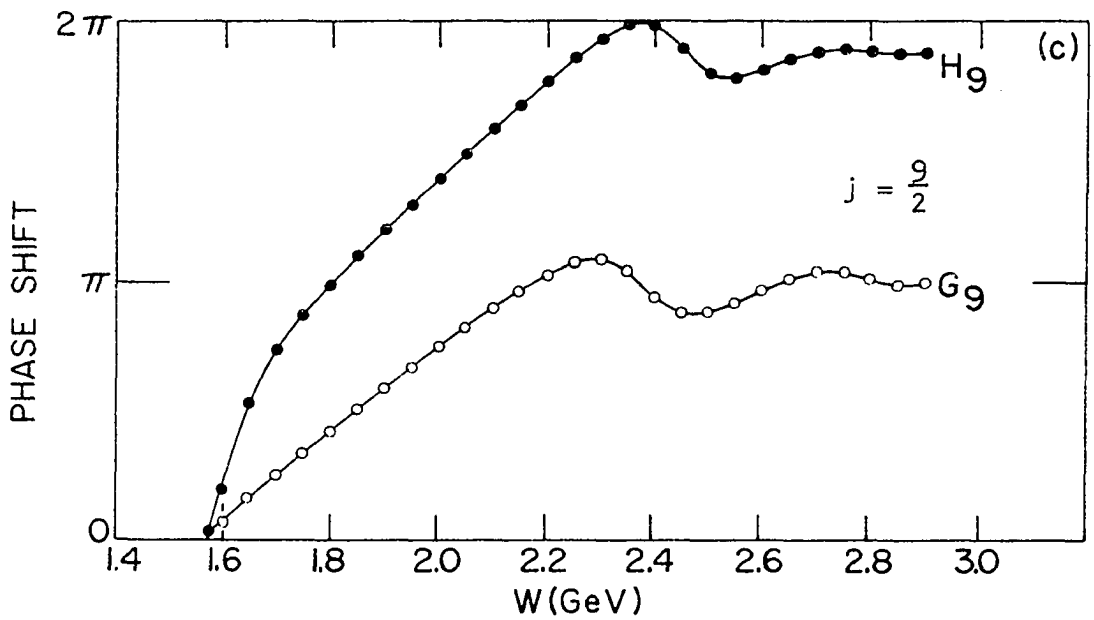
(c)
H9
j = 9/2
G9
PHASE SHIFT
2π
π
0
1.4
1.6
1.8
2.0
2.2
2.4
2.6
2.8
3.0
W(GeV)

Hence $r \to 0$ corresponds to a maximum in $|T_{\ell\pm}|$ and $r \to 1$ produces a minimum.

In Figs. 7 and 8 the positions of these maxima and minima are plotted in terms of L (or ℓ) versus M^2. Except for a few points in the low energy region, the trajectories obtained from the analysis are linear and show the parallel daughter structure similar to those obtained for mesons (23). As the value of L increases, the resulting Argand diagrams become more and more similar to the curve drawn for an inelastic scattering amplitude in Fig. 11. The curves for $j = \frac{9}{2}$ are shown in Fig. 6; the daughter structure results from the secondary loops seen at higher energies, which are seen as maxima and minima of $|T_{\ell\pm}|$. Included in Fig. 6c is the phase shift measured from the Real T_ℓ axis counterclockwise. As shown in Appendix C, there is an arbitrary phase of $\frac{\pi}{2}$ which can not be determined from the theory. This means that the phase shift, d_1+d_2, can be measured from any of the axes, and the values of these phase shifts in Fig. 6c should be considered to include this ambiguity. As is evident from the figure, the maxima and minima of the absolute value of the amplitude do not necessarily occur when the phase shift goes through $\frac{\pi}{2}$. Since the amplitudes may contain some non-resonating background which would add to the ambiguity already inherent in the phase shift, it was thought that the maxima and minima of $|T_{\ell\pm}|$ would serve as a more reliable indication of resonance structure than the phase shift method.

In order to compare with previous analyses, we have plotted in Fig. 9 all the points in a form exhibiting parity doubling (25) due to the MacDowell symmetry of the amplitudes (see Appendix A). Trajectories linear in W^2 correspond to parabolas in this plot, and the correspondence between our points, those obtained in π-N elastic (21) and those obtained in (22) for

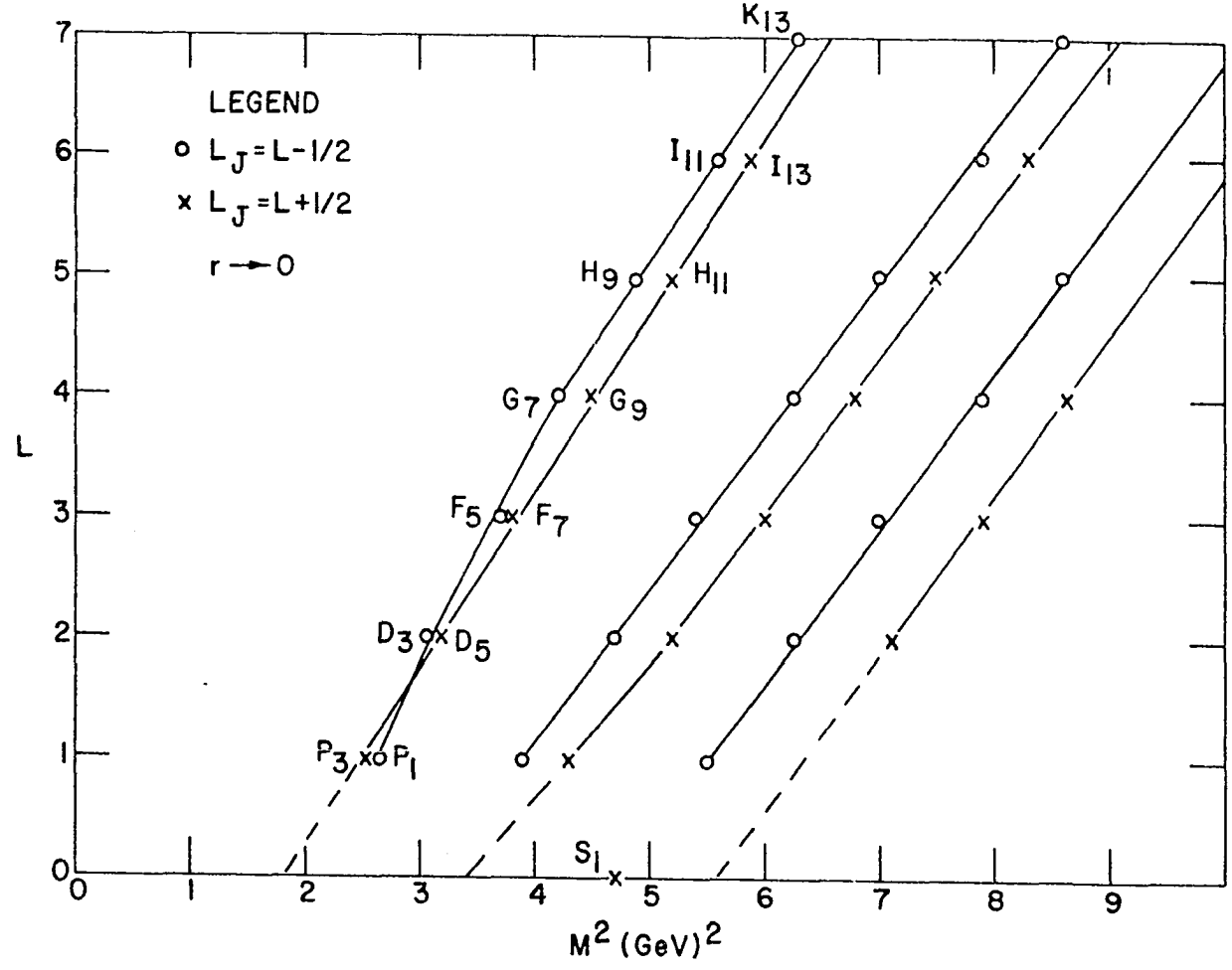

Fig. 7. Resonance Trajectories in Orbital Angular Momentum L versus M^2 for Absorptive Resonances

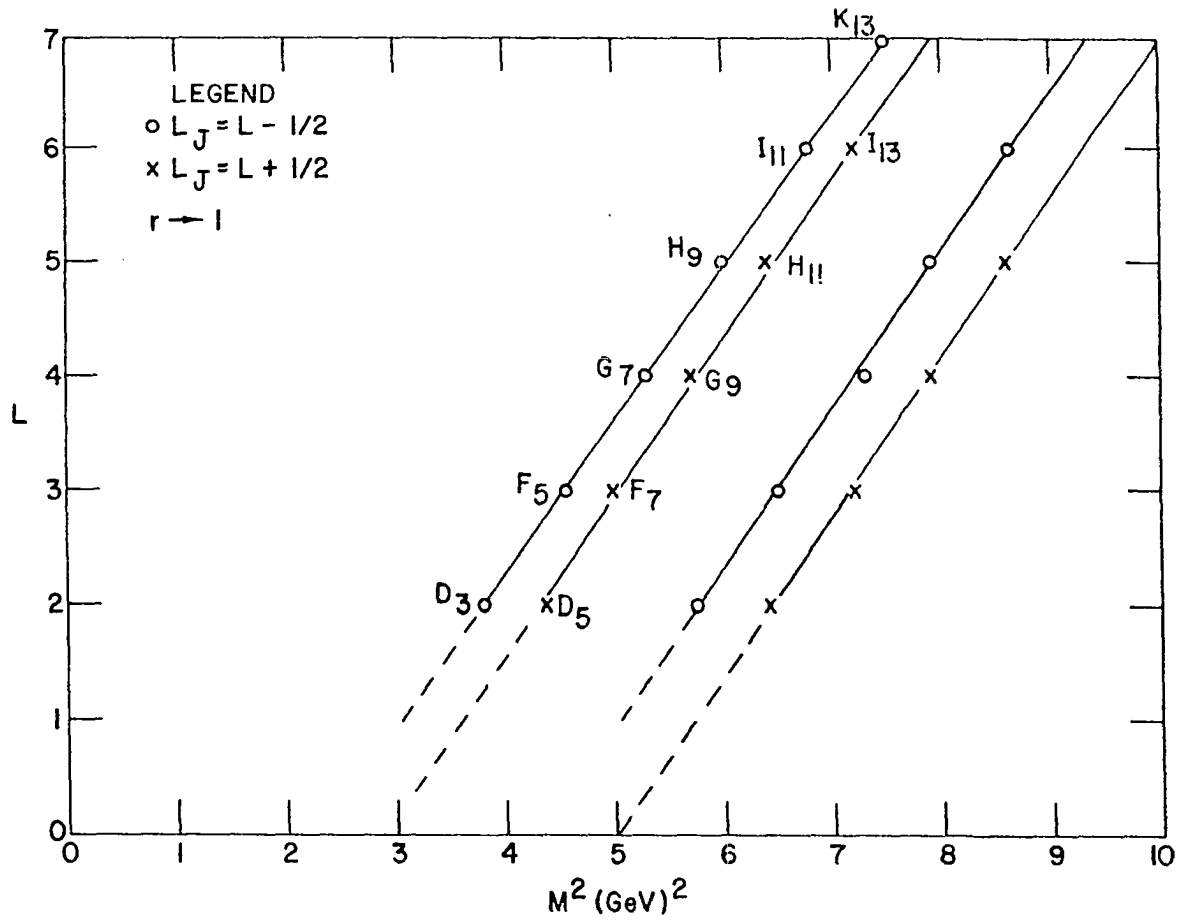

Fig. 8. Resonance Trajectories in Orbital Angular Momentum L versus M^2 for Elastic Resonances

Fig. 9. Plot of Parity-Doublet Baryon Trajectories

The circles correspond to the trajectories obtained from this calculation. The squares correspond to the resonance positions obtained in a similar calculation done for elastic π-N scattering by Collins, et al. (21). The crosses correspond to the resonance positions obtained from the phase shift analysis of the low energy data (22), most of which have been been observed experimentally as peaks in the total π-N elastic and charge exchange cross sections (25).

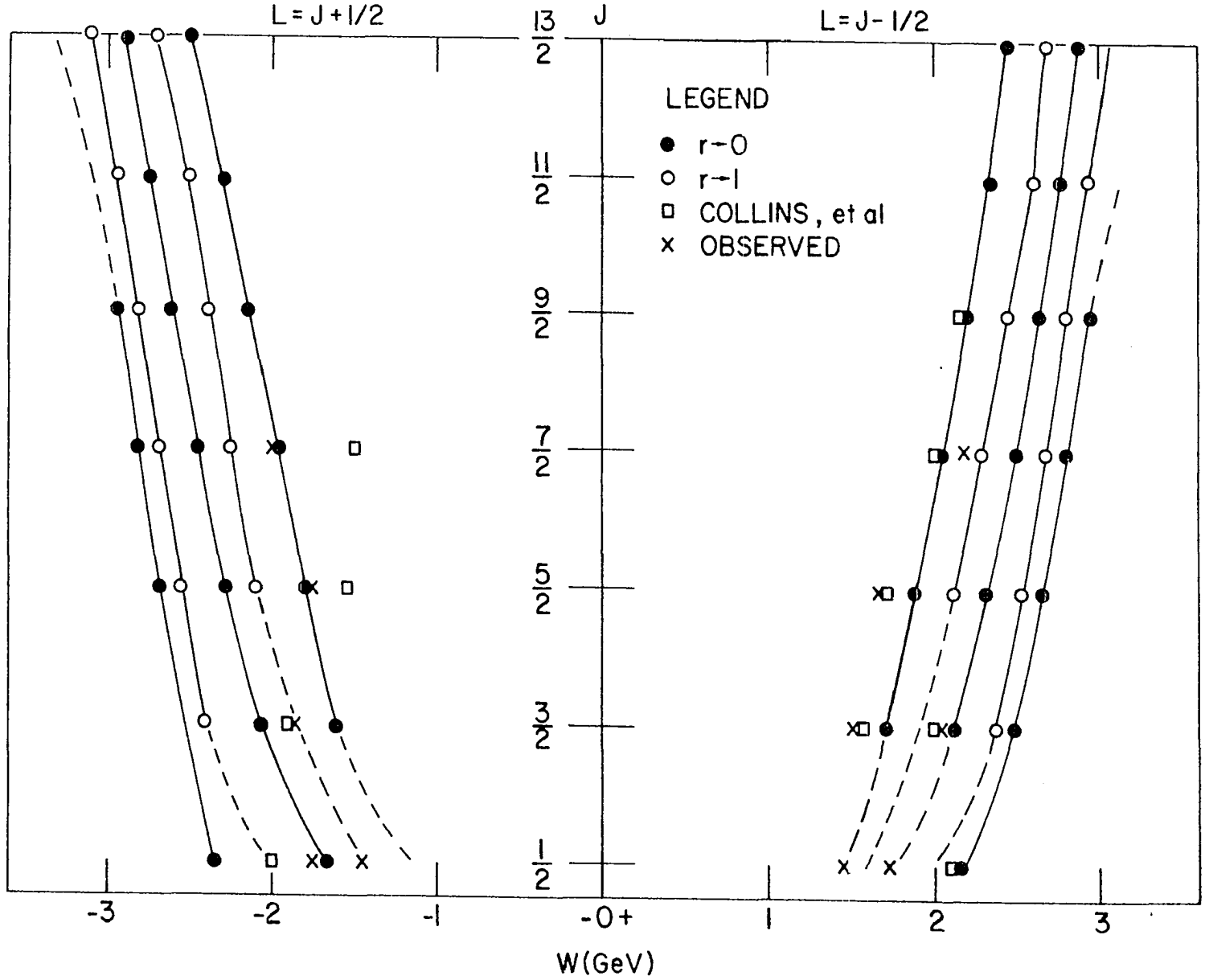
L = J + 1/2
L = J - 1/2
J
13/2
11/2
9/2
7/2
5/2
3/2
1/2
LEGEND
r-0
r-1
COLLINS, et al
OBSERVED
-3
-2
-1
-0+
1
2
3
W(GeV)

the phase shift analysis of the low energy data is fairly reasonable. The largest discrepancies are seen in the region $|W| \leq 1.6$ GeV, where we did not expect much accuracy from our amplitudes. The regularity of the resonance positions shown in the figures is one of features of the duality hypothesis subject to experimental check, as it seems to appear also in the meson bootstrap calculations (23), (24), and predicts the masses, spins and parities of a large number of resonance states.

A rather surprising result is the close correspondence between the theoretical shape of the Argand diagram for an inelastic amplitude, shown in Fig. 11, and the shapes obtained in this calculation, Fig. 6. The Regge analysis for π-N elastic scattering (21) produced circles corresponding closely to the theoretical shape of the Argand diagram for an elastic scattering amplitude. The primary difference between the two calculations is the difference in signature of the trajectories involved; the rho has negative signature, and the A_2 has positive. It is hard to understand how the change of signature produces this difference, but it seems significant that the calculated curves do differ in this special way.

Two other representations of the eta pion-production amplitudes were also analyzed. These were the single-pole fit by Arbab, et al. (26), and the double-pole fit by Austin, et al. (6). These amplitudes gave results very similar in form to those discussed above; the actual positions of the resonances were shifted a bit one way or the other. The source of complication in treating these amplitudes is the extremely poor fit to the low energy cross sections obtained with them. In fact, we were unable to obtain a reasonable fit to even the high energy cross sections using the

amplitudes of Arbab, et al. (26) because of an error in their published parameters. The amplitudes of Austin, et al. (6) give a reasonable fit for only a limited range of t (as was the original intention of the authors), and required some doctoring of the strong t-dependence before they could be used in the analysis. However, since the shape of the Argand diagrams obtained was very similar and the trajectories produced were very nearly linear in M^2 for all cases, only the case already presented here was studied in detail.

Table I gives a comparison of the results for the first few states found in the inelastic reaction with those found in the elastic reaction (21) and with those found in the phase shift analysis of the low energy data (22). As is evident from the table, we were not able to reproduce the lower energy states very well, whereas the agreement of the three calculations becomes more reasonable for the higher energy states. It should also be noted here that the analysis of the elastic case involved Regge amplitudes for the t-channel containing the P, P', and ρ trajectories, and amplitudes for the u-channel region (backward scattering) containing the N and Δ trajectories. A factor of $\sin \pi\alpha$ was incorporated into the residue functions in order to fit smoothly the behavior in the fitted ranges of t and u. This is in contrast to the present treatment wherein the t-channel amplitude is extrapolated over the entire range of t (for the physical s-channel), and a good "averaged" fit to the total cross section for all but the lowest energies is obtained (see Figs. 4 and 5). In spite of these differences, the results of the three calculations, including the shapes of the Argand diagrams as well as the resonance masses, are in remarkable agreement.

Table 1. Masses of Resonance States Found in Three Different Analyses

Partial Wave	This Calculation[a]	Elastic Case[b]	Phase Shift[c]
S_{11}	2150 (MeV)	2100 (MeV)	1535 (MeV)
	--	--	1750
P_{11}	1630	1450	1470
	1950	2000	1750
P_{13}	1600	1860	1863
	2050	--	--
D_{13}	1730	1550	1520
	2150	--	2057
D_{15}	1775	1700	1680
F_{15}	1900	1530	1690
F_{17}	1950	1500	1983
G_{17}	2050	2010	2200
G_{19}	2120	2150	--

[a] This calculation is a partial wave analysis of the amplitudes for eta pion-production.

[b] The elastic case is a similar analysis of π-N elastic scattering (21).

[c] The phase shift analysis (22) was done on the low energy elastic scattering data.

VI. APPENDIX

A. Partial Wave and Helicity Amplitudes and Kinematics

In this appendix some useful forms of the scattering amplitudes for the reaction

$$\pi^- + p \rightarrow \eta + n \qquad (6.1)$$

are derived using the notation of Gasiorowicz (27). These are the amplitudes required in Chapters IV and V.

The diagram in Fig. 10 shows the labeling of the particles and the ir momenta. The various channels are defined by

$$\text{s-channel:} \quad s = (k_1 + k_2)^2, \qquad \pi^- + p \rightarrow \eta + n \qquad (6.2)$$

$$\text{t-channel:} \quad t = (k_2 + k_4)^2, \qquad \bar{n} + p \rightarrow \pi^+ + \eta$$

$$\text{u-channel:} \quad u = (k_2 + k_3)^2, \qquad \bar{\eta} + p \rightarrow \pi^+ + n.$$

The center of mass scattering angles, θ_s and θ_t are defined in Fig. 10a, Fig. 10b and 10c. The physical momenta in the center of mass system are

$$\text{s-channel:} \quad k_1 = (\omega, \vec{q}), \qquad k_2 = (E, -\vec{q}) \qquad (6.3)$$

$$-k_3 = (\omega', \vec{q}'), \qquad -k_4 = (E', -\vec{q}').$$

$$\text{t-channel:} \quad k_4 = (E, \vec{p}), \qquad k_2 = (E, -\vec{p})$$

$$-k_1 = (\omega, -\vec{q}), \qquad -k_3 = (\omega', \vec{q}).$$

The helicity states are normalized covariantly:

$$\text{For spin zero bosons:} \quad \langle q' | q \rangle = 2\omega_q \, \delta^3(\vec{q}' - \vec{q}) \qquad (6.4)$$

$$\text{For fermions:} \quad \langle p', \lambda' | p, \lambda \rangle = \frac{E_p}{M} \, \delta_{\lambda', \lambda} \, \delta^3(\vec{p}' - \vec{p}).$$

With this normalization, the T-matrix, defined by

$$\langle f | \, S - 1 \, | i \rangle \equiv -(2\pi)^4 \, i \, \delta^4(p_f - p_i) \, T_{fi} \qquad (6.5)$$

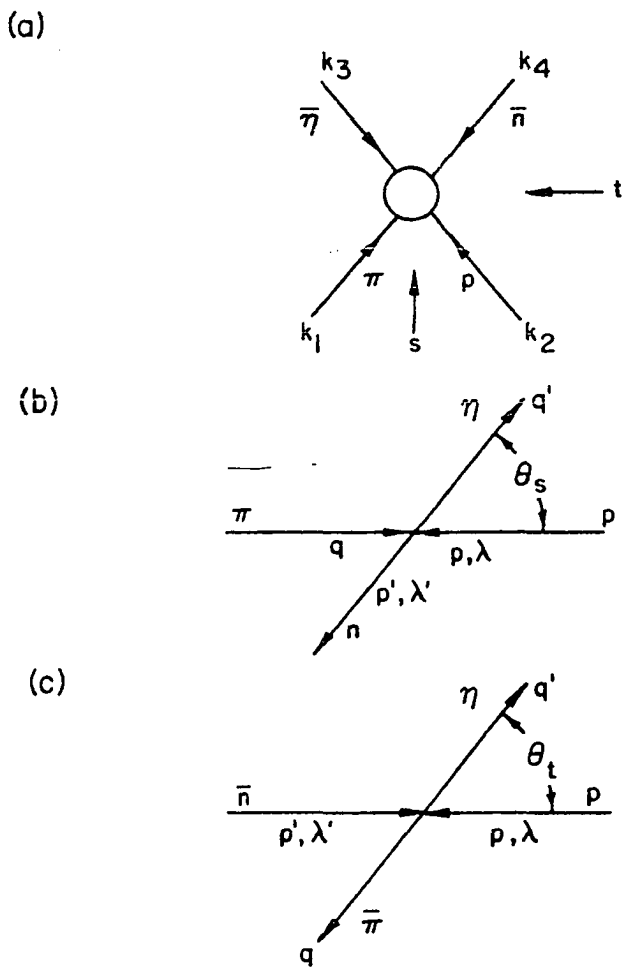

Fig. 10. Diagrams Defining Kinematic Variables

(a): Diagram defining Mandelstam variables.

(b): The s-channel kinematics in the center of mass system.

(c): The t-channel kinematics in the center of mass system.

is a Lorentz scalar. The differential cross section for reaction 6.1 is given by

$$d^6\sigma = \frac{(2\pi)^4 \delta^4(p_f - p_i)}{J} \; |T_{fi}|^2 \; \frac{d^3p'}{E'/M} \; \frac{d^3q'}{2\omega'} \qquad (6.6)$$

where the current density J is defined by the product of the densities of the initial states and the relative velocities of the incident particles,

$$J = \frac{2\omega}{(2\pi)^3} \; \frac{E}{(2\pi)^3 M} \; \left(\frac{|\vec{q}|}{2\omega} \; \frac{|\vec{p}|}{E}\right)$$

$$= (2\pi)^{-6} \frac{2q}{M} (E + \omega)$$

in the center of mass system. The particles states are normalized to one particle per unit volume. For the s-channel reaction, the total center of mass energy is given by

$$\sqrt{s} = W = E + \omega = E' + \omega'. \qquad (6.7)$$

The integration over d^3q' can be carried out by means of the delta function, and the resulting expression is

$$d^3\sigma = \frac{(2\pi)^{10} M^2}{2 q W} \; \frac{d^3p'}{E'} \; \delta[(p + q - p')^2 - m_3^2] \; \theta(p_o + q_o - p_o') \; |T_{fi}|^2.$$

The relation $d^3p' = p'^2 dp' \, d\Omega = p' E' dE' \, d\Omega$ determines the axis to which the scattering angle is referred. Carrying out the final integration over the delta function, we obtain

$$d^2\sigma = \frac{(2\pi)^{10} M^2}{2qW} \frac{p'}{2W} |T_{fi}|^2 \, d\Omega \, . \qquad (6.8)$$

Averaging over the initial spin states and summing over the final spin states gives the differential cross section for all possible final state spin configurations,

$$\frac{d\sigma}{d\Omega} = \frac{1}{2S_a+1}\,\frac{1}{2S_b+1}\,\frac{1}{4\pi^2 s}\,\frac{p'}{q}\sum_{cdab}\left|f^s{}_{cd;ab}(s,t)\right|^2 , \tag{6.9}$$

where

$$f^s{}_{cd;ab}(s,t) \equiv -(2\pi)^5\, M\, T_{cd;ab}$$

is the s-channel helicity amplitude defined by Wang (15), and the helicity notation has been simplified by taking $\lambda_1 = a, \lambda_2 = b, \lambda_3 = c,$ and $\lambda_4 = d$. These helicity amplitudes satisfy the relations

$$f_{cd;ab} = \zeta\, f_{-c\ -d;\ -a\ -b} \tag{6.10}$$

where

$$\zeta = \frac{\zeta_a\zeta_b}{\zeta_c\zeta_d}\,(-1)^{S_a+S_b-S_c-S_d}\,(-1)^{(a-b)\,-\,(c-d)};$$

the ζ's are the intrinsic parities of the particles,

$$\zeta_\pi = -1,\ \zeta_\eta = -1,\ \zeta_p = +1,\ \zeta_n = +1,$$

and the S's are their spins,

$$S_\pi = 0,\ S_\eta = 0,\ S_p = 1/2,\ S_n = 1/2.$$

These relations imply that there are only two independent helicity amplitudes for reaction 6.1,

$$f^s_{0+;\ 0+} = f^s_{0-;0-} \tag{6.11}$$

and

$$f^s_{0-;0+} = -\,f^s_{0+;0-}\ .$$

In terms of the four-momentum transfer t, the differential cross section is

$$\frac{d\sigma}{dt} = \frac{\pi}{qp'}\,\frac{d\sigma}{d\Omega} = \frac{1}{4\pi s q^2}\,\frac{1}{(2S_a+1)(2S_b+1)}\sum_{cdab}\left|f^s{}_{cd;ab}(s,t)\right|^2. \tag{6.12}$$

The invariant amplitudes for reaction 6.1, A and B, are defined by

$$T^{s}_{0d;0b} \equiv (16\pi)^{-5}\ \bar{u}(p',d)\{-A(s,t) + \not{Q}\, B(s,t)\}\ u(p,b), \qquad (6.13)$$

where $\not{Q} = \frac{1}{2}(q_a + q_c)^{\mu}\gamma_{\mu}$, and the u's are the four-component Dirac spinor nucleon wave functions. In the notation of Gasiorowicz (27),

$$u(-q\,\hat{\epsilon}_z, b) = (-1)^{S_b - b}\, e^{-i\pi\sigma_2/2}\, u(q\hat{\epsilon}_z, b) \qquad (6.14)$$

$$= [2M(E+M)]^{-1/2} \begin{pmatrix} E+M \\ 2bp \end{pmatrix} \chi_{-b}\ ,$$

$$u(-\vec{q}',d) = e^{i\theta\sigma_2/2}\, u(-q'\,\hat{\epsilon}_z, d)$$

$$= [2M(E+M)]^{-1/2} \begin{pmatrix} E'+M \\ 2dq' \end{pmatrix} (\cos\tfrac{\theta}{2} - i\,\sigma_2 \sin\tfrac{\theta}{2})\,\chi_{-d}\ .$$

Since $\bar{u} = u^{\dagger}\gamma_0$,

$$\bar{u}(-\vec{q}',d) = N'\,(E_+', -2dq')\,\chi_{-d}^{\dagger}\,(\cos\tfrac{\theta}{2} + i\,\sigma_2 \sin\tfrac{\theta}{2})\ , \qquad (6.15)$$

where we define

$$E_{\pm} = E \pm M = \frac{(W \pm M)^2 - m_a^2}{2W}\ , \qquad E'_{\pm} = E' + M = \frac{(W \pm M)^2 - m_c^2}{2W}\ ,$$

$$N = [2M(E+M)]^{-1/2}, \qquad N' = [2M(E'+M)]^{-1/2}\ .$$

The four-component wave functions are products of two two-dimensional vectors which are operated on by two sets of Pauli matrices, σ^{μ} and τ^{μ}. The σ's operate on the χ spinors and the τ's operate on the $(E, \vec{\sigma}\cdot\vec{p})$ spinors. In this notation,

$$\not{Q} = Q_o\tau_3 - \vec{\gamma}\cdot\vec{Q} = Q_o\tau_3 - i\,\tau_2\,\vec{\sigma}\cdot\vec{Q}$$

$$= \tfrac{1}{2}(\omega + \omega')\,\tau_3 - \tfrac{i}{2}\tau_2[\sigma_1\, q' \sin\theta + \sigma_3(q + q'\cos\theta)].$$

The helicity amplitudes take the form

$$f^{s}_{0d;0b} = -2\pi MNN' \{ (E'_{+}, -2dq') \chi_{-d}^{\dagger} (\cos\frac{\theta}{2} + i\sigma_2 \sin\frac{\theta}{2}) \quad (6.16)$$

$$\times[-A + \frac{1}{2}(\omega + \omega')\tau_3 B$$

$$-\frac{i}{2}\tau_2\langle \sigma_1 q' \sin\theta + \sigma_3 (q + q'\cos\theta)\rangle B] \begin{pmatrix} E_+ \\ 2bq \end{pmatrix} \chi_{-b} \}.$$

The relations

$$\chi_{-d}^{\dagger} \chi_{-b} = \delta_{db}$$

$$\chi_{-d}^{\dagger} i\sigma_2 \chi_{-b} = (-1)^{1/2 - b} \delta_{d,-b}$$

$$\chi_{-d}^{\dagger} \sigma_1 \chi_{-b} = \delta_{d,-b}$$

$$\chi_{-d}^{\dagger} \sigma_3 \chi_{-b} = (-1)^{1/2 + b} \delta_{db}$$

inserted into 6.16 give

$$f^{s}_{od;ob} = -2\pi MNN'\{[(E_+'E_+ - 4dbqq') (-A) + \frac{1}{2}(\omega + \omega')(E_+'E_+ + 4dbqq') B]$$

$$\times[\cos\frac{\theta}{2}\delta_{d,b} + \sin\frac{\theta}{2}(-1)^{1/2-b}\delta_{d,-b}]$$

$$-\frac{1}{2} B (2bp E_+' + 2dp' E_+)[\cos\frac{\theta}{2}\langle q' \sin\theta \delta_{d,-b}$$

$$+ (q + q'\cos\theta)(-1)^{1/2 + b}\delta_{d,b}\rangle + \sin\frac{\theta}{2}\langle q'\sin\theta$$

$$\times(-1)^{1/2 + b}\delta_{d,b} - (q + q'\cos\theta)\delta_{d,-b}\rangle]\} \quad (6.17)$$

Using the relations

$$\omega + \omega' = W - E + W - E' = 2(W + M) - E_+' - E_+,$$

and

$$q + q' = (E_+E_-)^{1/2} + (E_+'E_-')^{1/2},$$

we find the two independent helicity amplitudes

$$f^{s}_{o+;0+} = -\pi \cos\frac{\theta}{2}\{(E_+'E_+)^{1/2}[-A + (W-M)B] \qquad (6.18)$$
$$-(E_-'E_-)^{1/2}[-A - (W+M)B]\}$$
$$= \pi \cos\frac{\theta}{2}(f_1 + f_2),$$

and

$$f^{s}_{0-;0+} = \pi \sin\frac{\theta}{2}(f_1 - f_2),$$

where

$$f_1 = (E_+'E_+)^{1/2}[A - (W-M)B], \qquad (6.19)$$

$$f_2 = (E_-'E_-)^{1/2}[-A-(W+M)B].$$

In terms of the invariant amplitudes of CGLN (28), A^c and B^c,

$A = \frac{1}{4\pi}A^c$, $B = \frac{1}{4\pi}(-B^c)$, which gives

$$f_1 = \frac{1}{4\pi}(E'+M)^{1/2}(E+M)^{1/2}[A^c + (W - M)B^c] \qquad (6.20)$$

$$f_2 = \frac{1}{4\pi}(E'-M)^{1/2}(E-M)^{1/2}[-A^c + (W + M)B^c].$$

The amplitudes with definite total angular momentum, $j = \ell \pm \frac{1}{2}$, and definite parity, $P = (-1)^{\ell+1}$, are given by

$$f_{\ell\pm} = \frac{1}{q}e^{i\delta_{\ell\pm}}\sin\delta_{\ell\pm} \qquad (6.21)$$
$$= \frac{1}{4qW}\int_{-1}^{1}(f_1 P_\ell(z) + f_2 P_{\ell\pm1}(z))\,dz \ .$$

It is evident from 6.20 and the definitions of $E_\pm$ in 6.15 that

$f_1(-W) = -f_2(W)$, which leads to the MacDowell symmetry relation (14),

$$f_{\ell,+}(W) = -f_{\ell+1,-}(-W). \qquad (6.22)$$

In order to carry out the Argand analysis and to determine the kinematic singularities in t of the helicity amplitudes used in Chapter IV, the t-channel helicity amplitudes must be found in terms of the invariant amplitudes, A and B. This is done by continuing the expression 6.13 for $T^{s}_{cd;ab}$ to the t-channel physical region, using the notation in Fig. 10c, and substituting for the outgoing nucleon spinor $\bar{u}$ an expression for an incoming antinucleon, $\bar{v}$, defined by

$$\bar{v}(p',d) = N(2dp', -E_+)\chi_d^{\dagger}. \tag{6.23}$$

With these phase conventions for the spinors, the helicity amplitudes take the form

$$f^{t}_{00;db} = (-1)^{1/2-d}(-2\pi M)\,\bar{v}(p',d)\left[-A + \tfrac{1}{2}(q'-q)^{\mu}\gamma_{\mu} B\right] u(p,b) \tag{6.24}$$

$$= (-1)^{1/2-d}\frac{\pi}{E_+}(-2dp, -E_+)\chi_{-d}^{\dagger}\left[-A + \tfrac{1}{2}(q'-q)^{\mu}\gamma_{\mu}B\right]\begin{pmatrix} E_+ \\ 2bp \end{pmatrix}\chi_{-b}$$

$$= -(-1)^{1/2-d}\frac{\pi}{E_+}\{pE_+\delta_{d,b}\left[(2d+2b)A + \tfrac{1}{2}(\omega'-\omega)(-2d+2b)B\right]$$

$$+B(4dbp^2-E_+^2)\left[q\sin\theta_t\delta_{d,-b} + q\cos\theta\,(-1)^{1/2+b}\delta_{d,b}\right]\}.$$

The two independent t-channel helicity amplitudes are

$$f^{t}_{00;++} = f^{t}_{00;--} = -2\pi(pA + Mq\cos\theta_t B), \tag{6.25}$$

$$= -\tfrac{1}{2}(pA^{c} - Mq\cos\theta_t B^{c})$$

and

$$f^{t}_{00;+-} = -f^{t}_{00;-+} = 2\pi Eq\sin\theta_t B,$$

$$= -\tfrac{1}{2}Eq\sin\theta_t B^{c}.$$

The kinematic factors are given in terms of the Mandelstam variables by

$$p = \frac{\{t - (m_b-m_d)^2\}^{1/2}\{t - (m_b+m_d)^2\}^{1/2}}{2\sqrt{t}},$$

$$= \frac{1}{2}(t - 4M^2)^{1/2} \quad \text{for } m_b = m_d = M,$$

$$q = \frac{\{t-(m_a-m_c)^2\}^{1/2}\{t-(m_a+m_c)^2\}^{1/2}}{2\sqrt{t}},$$

$$t \equiv (2E)^2,$$

$$\Phi(s,t,u) = stu - s(m_a^2-m_c^2)(m_b^2-m_d^2) - t(m_a^2-m_b^2)(m_c^2-m_d^2)$$
$$- (m_a^2m_d^2-m_b^2m_d^2)(m_a^2-m_b^2-m_c^2+m_d^2),$$

$$= stu - t(m_\pi^2-M^2)(m^2-M^2) - M^2(m^2-m_\pi^2)^2 \qquad \text{for 6.1,}$$

where $s + t + u = \sum_i m_i^2$,

$$\cos\theta_t = \frac{t(s-u) + (m_a^2 - m_c^2)(m_b^2 - m_d^2)}{4t\,pq},$$

$$= \frac{s-u}{4pq} \qquad \text{for } m_b = m_d = M,$$

$$\sin\theta_t = \frac{2(t\Phi)^{1/2}}{4tpq},$$

$$\Phi^{1/2} = 2\sqrt{t}\,pq\sin\theta_t.$$

Writing 6.25 in terms of the Mandelstam variables, we obtain

$$f^t_{00;++} = -\frac{1}{4}(t-4M^2)^{-1/2}\{(t-4M^2)A^c - M(s-u)\,B^c\} \qquad (6.26)$$

$$= (t-4M^2)^{-1/2}\,\bar{f}^t_{++},$$

$$f^t_{00;-+} = \frac{1}{4}(t-4M^2)^{-1/2}\,\Phi^{1/2}\,B^c$$

$$= (t-4M^2)^{-1/2}\,\Phi^{1/2}\,\bar{f}^t_{-+},$$

where

$$\bar{f}^t_{++} = -\frac{1}{4}\{(t-4M^2)\ A^c - M(s-u)\ B^c\} \tag{6.27}$$

and

$$\bar{f}^t_{-+} = \frac{1}{4}\ B^c$$

are the kinematic singularity free, parity conserving helicity amplitudes (KSFPCHA) which are Reggeized in Chapter IV.

Inverting 6.27, we obtain

$$A^c = \frac{-4}{t-4M^2}\{\bar{f}^t_{++} - M(s-u)\ \bar{f}^t_{-+}\} \tag{6.28}$$

$$B^c = 4\ \bar{f}^t_{-+}.$$

The relations 6.28, inserted into the expression for f_1 and f_2 in 6.19, allow the partial wave analysis in 6.21 to be carried out, relating the t-channel Regge poles to the direct channel resonances which appear in $f_{\ell\pm}$.

B. Reggeization of Helicity Amplitudes

The procedure for Reggeizing helicity amplitudes as developed by Gell-Mann, et al. (14), is briefly outlined here for the sake of completeness.

The F-matrix is defined in terms of the S-matrix by

$$F_{fi} = (S_{fi} - \delta_{fi})\ (2i)^{-1}\ k_f^{-1/2}\ k_i^{-1/2},$$

where k is the center of mass momentum. In terms of the Jacob-Wick helicity amplitudes (16), the scattering amplitudes for zero azimuthal angle are defined by

$$f_{cd;ab} = k_f^{1/2} k_i^{-1/2} \sum_j (2j+1) \langle c,d|F^j|a,b\rangle \, d^j_{\alpha\beta}(\theta) \tag{6.29}$$

where $\alpha = a-b$, $\beta = c-d$ and

$\langle c,d|F^j|a,b\rangle \equiv \langle jm,c,d|F|jm,a,b\rangle$.

When parity is conserved it is useful to define amplitudes of definite parity by

$$F^{j\pm}_{cd;ab} \equiv F^j_{cd;ab} \pm \zeta_c\zeta_d \, (-1)^{S_c+S_d-v} \, F^j_{-c-d;ab} \tag{6.30}$$

where ζ_i is the intrinsic parity and S_i is the spin of particle i, and $v = \frac{1}{2}$ for half-integral j and 0 for integral j. Parity-conserving scattering amplitudes are defined by

$$f^{\pm}_{cd;ab} \equiv (\sqrt{2}\cos\tfrac{\theta}{2})^{-|\alpha+\beta|}(\sqrt{2}\sin\tfrac{\theta}{2})^{-|\alpha-\beta|} \, f_{cd;ab}(z) \tag{6.31}$$

$$\pm(-1)^{\alpha+\alpha_m}\zeta_c\zeta_d(-1)^{S_c+S_d-v}(\sqrt{2}\sin\tfrac{\theta}{2})^{-|\alpha+\beta|}(\sqrt{2}\cos\tfrac{\theta}{2})^{-|\alpha-\beta|}$$

$$\times f_{-c-d;ab}(z)$$

where $\alpha_m = \max(|\alpha|,|\beta|)$ and $z = \cos\theta$. By defining new functions

$$e^{j\pm}_{\alpha\beta}(z) \equiv \tfrac{1}{2}(\sqrt{2}\cos\tfrac{\theta}{2})^{-|\alpha+\beta|}(\sqrt{2}\sin\tfrac{\theta}{2})^{-|\alpha-\beta|} \, d^j_{\alpha\beta}(\theta) \tag{6.32}$$

$$\pm\tfrac{1}{2}(-1)^{\alpha+\alpha_m}(\sqrt{2}\sin\tfrac{\theta}{2})^{-|\alpha+\beta|}(\sqrt{2}\cos\tfrac{\theta}{2})^{-|\alpha-\beta|} \, d^j_{\alpha\,-\beta}(\theta) \quad ,$$

we can write the parity conserving helicity amplitudes in the form

$$f^{\pm}_{cd;ab} = \frac{k_f^{1/2}}{k_i^{1/2}} \sum_j (2j+1) \{e^{j+}_{\alpha\beta}(z) \, F^{j\pm}_{cd;ab} + e^{j-}_{\alpha\beta}(z) \, F^{j\mp}_{cd;ab}\}. \tag{6.33}$$

The general expression for the e^j's for integral j and non-negative α and β in terms of derivatives of Legendre polynomials, P_j, is

$$e^{j}_{\alpha\beta}(z) = (-1)^{\alpha}\,[\,(j-\alpha)!\,(j-\beta)!\,/\,(j+\alpha)!\,(j+\beta)!\,] \tag{6.34}$$

$$\times D^{|\alpha-\beta|}\times(D^2 - D - zD^2)^m\, P_j(z),$$

where $D = \frac{d}{dz}$, $m = \min(|\alpha|, |\beta|)$, and $e^{j}_{00} = P_j$.

In order to investigate the properties of these amplitudes, Gell-Mann, et al. (14), give a heuristic discussion in which such questions as j-plane cuts, fixed poles and essential singularities are ignored. In the spinless case, they start with the expansion

$$f(z) = \sum_{j=0}^{\infty} (2j+1)\, F^j\, P_j(z), \tag{6.35}$$

and the Froissart inversion formula,

$$F^j = \int dz\, \omega(z)\, Q_j(x), \tag{6.36}$$

where $\omega(z)$ is the weight function of $f(z)$ in a dispersion relation in z. Since Q_j has fixed poles for j a negative integer, some procedure for avoiding these must be found. The relation

$$P_j = \frac{1}{\pi} \tan \pi j\, (Q_j - Q_{-j-1}) \tag{6.37}$$

suggests that the fixed poles can be avoided by defining

$$R_j \equiv -\frac{1}{\pi} \tan \pi j\, Q_{-j-1} \tag{6.38}$$

$$= \pi^{-1/2}\, \Gamma(j + \tfrac{1}{2})/\Gamma(j+1)\ \ (2z)^j\, F(-j/2,\ 1/2-j/2;\ 1/2-j;\ z^{-2}).$$

At $j = 0, 1, 2, \ldots$, $R_j = P_j$ and at $j = -1, -2, \ldots$, $R_j = 0$. Since F^j is finite at negative integral j by assumption, the sum can be extended to all j:

$$f(t,z) = \sum_{j=-\infty}^{+\infty} (2j+1)\, F^j(t)\, R_j(z). \tag{6.39}$$

The summation is converted to a contour integral by the Sommerfeld-Watson transform,

$$f(t,z) = \frac{1}{2\pi i} \oint (2j+1) \frac{F^j(t)}{\sin \pi j} \; R_j(-z), \tag{6.40}$$

where the contour encloses the entire real axis. The $R_j(z)$ have poles at the half-integers which are canceled as follows: The factor $(2j+1)$ cancels the pole at $j = -1/2$; from the Froissart inversion 6.36, $F^j = F^{-j-1}$ at half-integral j, and the residues of

$$(2j+1)\ \pi \frac{F^j}{\sin \pi j} R_j(-z)$$

at half-integral j and $-j-1$ are equal and opposite, thus cancelling the poles. The contour is expanded to infinity, and it is assumed that only moving poles are picked up in the complex j-plane; furthermore, the poles are assumed to dominate any contribution from the background integral. A pole in F^j of the form $\beta(t)\ (j - \alpha)^{-1}$ gives a contribution to $f(t,z)$ equal to

$$-(2\alpha+1)\ \pi \frac{\beta}{\sin \pi\alpha} \; R_j(-z).$$

If a moving pole passes through a value $\alpha = j_o$, for $j_o = 1/2, 3/2, \ldots$, at some energy t_o, then unless the residue vanishes there, the relation $F^j = F^{-j-1}$, j half-integral, implies that another trajectory α' must pass through $-j_o-1$ at the same energy with equal and opposite residue, compensating for the pole at that energy.

To extend this method to the case including the effects of spin, the functions $E^{j\pm}_{\alpha\beta}(z)$ are defined by replacing the P_j in the definition of $e^j_{\alpha\beta}$, Equation 6.34, by $R_j(z)$. For $j = 1, 2, 3, \ldots$, $e^{j\pm}_{\alpha\beta} = E^{j\pm}_{\alpha\beta}(z)$. For $j = -2, -3, \ldots$, $E^{j\pm}_{\alpha\beta} = 0$, and $F^{j\pm}$ are finite, so the sum may be extended to these values. For $j = 0, -1$, however, it is shown (14) that

$F^{0\pm}_{\mp} = F^{(-1)\mp}$ and $E^{0\pm}_{\mp} = E^{(-1)\mp}$, so that these terms cancel in the partial wave sum. Thus the partial wave sum

$$f^{\pm}_{cd;ab} = \sum_{j=-\infty}^{+\infty} (2j+1) \{E^{j+}_{\alpha\beta} F^{j\pm}_{cd;ab} + E^{j-}_{\alpha\beta} F^{j\mp}_{cd;ab}\} \tag{6.41}$$

may be extended to a contour integral as in 6.40, and the poles at half-integral j are cancelled as before, with $F^{j\pm}_{\mp} = F^{(-j-1)\pm}_{\mp}$ for j half-integral. The contributions from the Regge poles take the form

$$f^{\pm}_{\mp}(t,z) \sim \frac{(2\alpha_{\pm}+1)}{\sin \pi\alpha_{\pm}} E^{(\alpha_{\pm})}_{\mp} {}_{\alpha\beta}(z)\, \beta_{\pm}(t) - \frac{(2\alpha_{\mp}+1)}{\sin \pi\alpha_{\mp}} E^{(\alpha_{\mp})}_{\pm} {}_{\alpha\beta}(-z)\, \beta_{\mp}{}_{\pm},$$

from the trajectories α_+ and α_- corresponding to poles in F^{j+} and F^{j-}.

For this amplitude a new type of compensation has appeared which can be understood in the following way. A channel is referred to as a "nonsense" channel when $j \sim \alpha = a-b$ or $j < \beta = c - d$, since that value of j is not reached physically. If $j > \alpha$ or $j > \beta$, then that channel is called a "sense" channel, and one expects to find a physical particle for that particular value of j at the energy for which the trajectory passes through j. The possible combinations of residue functions are defined by

$$\beta^{j}_{cd;ab} = \begin{cases} \beta_{ss} \text{ for } |a-b| \text{ and } |c-d| < j; \\ \beta_{sn} \text{ for } |c-d| < j < |a-b|; \\ \beta_{nn} \text{ for } j < |a-b| \text{ and } |c-d|. \end{cases} \tag{6.42}$$

These are called sense-sense (β_{ss}), sense-nonsense (β_{sn}), and nonsense-nonsense (β_{nn}) amplitudes. Consider a trajectory $\alpha_{\pm}$ passing thru $j = 0$ for a certain value of the energy in an amplitude with $|a-b| = |c-d| = 1$. If the trajectory chooses sense at $j = 0$, $\beta^{\pm}_{11}$ must vanish like $\alpha_{\pm}$ as $\alpha_{\pm} \to 0$ so that no "ghost" state appears (i. e., a state with physical spin

$j = 0$, but negative mass, $\sqrt{t_o}$). However, if the trajectory $\alpha^{\pm}$ chooses nonsense at $\alpha^{\pm} = 0$, then $\beta^{\mp}_{11}$ is non-zero there and the "ghost" must be compensated for ("killed") by some other mechanism, since the physical amplitudes cannot have a singularity at a nonsensical value of j. This cancellation is accomplished by a compensating trajectory with opposite parity, $\alpha^{\mp}_{+}$, which passes through $\alpha^{\mp}_{+} = -1$ at the same energy for which $\alpha^{\pm}$ passes through zero. Since

$$F^{(0)\pm} = F^{(-1)\mp} \text{ and } E^{(0)\pm}_{11} = E^{(-1)\mp}_{11},$$

the trajectories cancel each other, leaving $f^{\pm}$ finite.

This example is generalized to any integral value of $|a-b|$ and $|c-d|$ in the following manner. The values j_o of j ($j_o = 0, 1, \ldots, \min[|a-b|, |c-d|]$) for which we have a nonsense-nonsense transition compensate for the corresponding terms with $j = -j_o - 1$. For all relevant values of j_o, we have

$$E^{j_o\pm}_{\alpha\beta} = E^{(-j_o-1)\mp}_{\alpha\beta} \text{ and } F^{j_o\pm} = F^{(-j_o-1)\mp},$$

where the leading terms in $E^{j+}_{\alpha\beta}$ at large z vanish as $j = j_o$ down to a term of the right behavior to compensate the leading terms in $E^{(-j_o-1)-}_{\alpha\beta}$. For half-integral values of $|a-b|$ and $|c-d|$, the compensation for the relevant pairs of integral j occurs without a change in the parity index, leaving β_{nn} finite at these nonsense points.

A rather complete discussion of the various ghost-killing mechanisms is given by L. Bertocchi (25). A brief summary of this treatment is included here for completeness.

Since the residue functions β_{ss}, β_{sn}, β_{nn} are assumed to be factorizable (i. e., they are the products of two terms referring to the two

different vertices, (c,d) and (a,b)), they are constrained to satisfy

$$(\beta_{sn})^2 = \beta_{ss}\,\beta_{nn}. \tag{6.43}$$

This condition is important in determining the singularity structure of residue functions.

An example of the effects of the various ghost-killing mechanisms is elastic nucleon-nucleon scattering, in which all three kinds of amplitudes occur. In this case, we define

$$T_{++;++} = T_{ss} \quad \text{(no helicity flip)}, \tag{6.44}$$

$$T_{+-;++} = T_{sn} \quad \text{(helicity flip in one vertex)},$$

$$T_{+-;-+} = T_{nn} \quad \text{(double helicity flip)}.$$

By investigating the behavior of the E^j functions near nonsense points, we can determine the behavior of the amplitudes to be

$T_{ss} \sim \beta_{ss}\,\epsilon_\alpha$, $T_{sn} \sim \frac{\sqrt{\alpha}}{(\alpha+1)^{1/2}}\,\beta_{sn}\,\epsilon_\alpha$, and $T_{nn} \sim \frac{\alpha}{\alpha+1}\,\beta_{nn}\,\epsilon_\alpha$, where $\epsilon_\alpha = (1 \pm e^{-i\pi\alpha})/\sin\pi\alpha$, and the $\pm$ is determined by the signature, $(-1)^S$, of the Regge trajectory involved.

A right signature integer is an integer value of α which has the same parity as the values of the angular momentum for which physical particles actually appear on the trajectory. Wrong signature points are those which have the wrong parity. At a right signature point, $\epsilon_\alpha \sim \alpha^{-1}$, and at a wrong signature point, $\epsilon_\alpha \sim$ constant. Consider the behavior of the amplitudes near $t = t_o$, where $\alpha(t_o) = 0$. The amplitude T_{sn} contains a factor $\alpha^{1/2}$ which must be cancelled if a branch point at $t = t_o$ is to be avoided. Since there is no general reason to expect a branch point there, we can kill the singularity and satisfy factorization, 6.43, by taking

$$\beta_{ss} \sim 1,\ \beta_{sn} \sim \{\alpha(\alpha+1)\}^{1/2},\ \text{and}\ \beta_{nn} \sim \alpha(\alpha+1), \tag{6.45}$$

which is called the sense-choosing mechanism; an alternative choice is

$$\beta_{ss} \sim \alpha(\alpha+1),\ \beta_{sn} \sim \{\alpha(\alpha+1)\}^{1/2},\ \text{and}\ \beta_{nn} \sim 1, \tag{6.46}$$

which is called the Gell-Mann mechanism, and was discussed earlier. If the point in question is a right signature point, however, the sense-choosing mechanism leaves T_{ss} with a pole at $\alpha(t=t_o) = 0$; if $t_o < 0$, this would imply the existence of a particle with spin $\alpha(t_o)$ and imaginary mass, $\sqrt{t_o}$ (a ghost). Also, the form of the T_{nn} amplitude comes from the leading term in s; the mirror reflected term around $\alpha = -1/2$, which behaves like $s^{-\alpha-1}$, does not contain the factor α, and the Gell-Mann mechanism leaves a pole in this non-asymptotic term which must be removed by a compensating trajectory.

Another way to remove these difficulties is to multiply each of the factors in 6.45 and 6.46 by another factor of α. This leads to

$$\beta_{ss} \sim \alpha,\ \beta_{sn} \sim \alpha\{\alpha(\alpha+1)\}^{1/2},\ \text{and}\ \beta_{nn} \sim \alpha^2(\alpha+1), \tag{6.47}$$

which is called the Chew mechanism, or

$$\beta_{ss} \sim \alpha^2,\ \beta_{sn} \sim \alpha\{\alpha(\alpha+1)\}^{1/2},\ \text{and}\ \beta_{nn} \sim \alpha(\alpha+1), \tag{6.48}$$

which is called the non-compensating mechanism. In the non-compensating mechanism, there is no ghost even in the non-asymptotic term and no compensating trajectory is required. However, if a compensating trajectory is not there, the non-asymptotic term, which behaves as $s^{-\alpha-1}$, dominates the leading term s^{α} at $\alpha = 0$, since T_{ss}, T_{sn}, and the leading term of T_{nn} vanish there. Other possibilities of extra factors of α simply change the manner in which the amplitudes vanish and would be difficult to distinguish experimentally from 6.47 and 6.48.

The choice of a ghost-killing mechanism is a dynamical question which must be decided by phenomenological analysis. In the angular distribution for the reaction $\pi^- + p \rightarrow \pi^o + n$, the sense-choosing mechanism for the ρ trajectory forces T_{sn} to vanish at $t = -0.6$ $(GeV/c)^2$, while T_{ss} remains finite there ($\alpha = 0$ is a wrong signature point for the ρ, so there is no ghost there). The presence of a large dip at that value of t in the angular distribution favors this mechanism. The absence of a similar dip in $\pi^- + p \rightarrow \eta + n$ angular distribution, in which the A_2 trajectory is exchanged, favors the Gell-Mann mechanism. This leaves both T_{ss} and T_{sn} finite at $\alpha = 0$ (a right signature point for the A_2), and produces no dips in the angular distribution.

Other applications of ghost-killing mechanisms are reviewed in (25).

C. The General Form of the Three-Channel Scattering Matrix

In order to investigate the properties of an inelastic reaction, one must consider at least a three channel S-matrix describing an elastic channel, the inelastic channel of interest, and a third channel representing all the remaining channels, open or closed. Assuming only unitarity and symmetry (from time-reversal invariance), we find that the general S-matrix for the three channel case has six independent parameters and that the off-diagonal phase shifts are not, in general, factorizable. The additional assumption of factorizability of the phase shifts of the inelastic terms reduces the number of independent parameters to five and affords a simplification in the form of these off-diagonal elements. This assumption is essentially the requirement that the elastic channel resonances must also occur in the inelastic channels. We regard this as a physically reasonable hypothesis.

To find the general form of a 3x3 symmetric unitary matrix we need only consider a general unitary matrix in the representation usually considered useful in treating SU(3) (29). Labelling the generators of the Lie algebra by

$$\{J_i\} = \{T_1 = \frac{1}{2}\begin{pmatrix} 0 & 1 & 0 \\ 1 & 0 & 0 \\ 0 & 0 & 0 \end{pmatrix},\ T_2 = \frac{1}{2}\begin{pmatrix} 0 & i & 0 \\ -i & 0 & 0 \\ 0 & 0 & 0 \end{pmatrix},\ T_3 = \frac{1}{2}\begin{pmatrix} 1 & 0 & 0 \\ 0 & -1 & 0 \\ 0 & 0 & 0 \end{pmatrix}, \qquad (6.49)$$

$$U = \frac{1}{3}\begin{pmatrix} 1 & 0 & 0 \\ 0 & 1 & 0 \\ 0 & 0 & -2 \end{pmatrix}\},$$

$$\{K_i\} = \{N = \begin{pmatrix} 0 & 0 & 1 \\ 0 & 0 & 0 \\ 1 & 0 & 0 \end{pmatrix},\ N' = \begin{pmatrix} 0 & 0 & i \\ 0 & 0 & 0 \\ -i & 0 & 0 \end{pmatrix},\ M = \begin{pmatrix} 0 & 0 & 0 \\ 0 & 0 & 1 \\ 0 & 1 & 0 \end{pmatrix},$$

$$M' = \begin{pmatrix} 0 & 0 & 0 \\ 0 & 0 & i \\ 0 & -i & 0 \end{pmatrix}\},$$

we can use a theorem quoted by Hermann (30) which states that any connected Lie group G which only has a finite center and has a connected subgroup $\{J_i\}$ has the "almost unique" decomposition

$g = k \cdot j,$

where $k = e^{iaK}$ and $j = e^{ibJ}$. This decomposition is "almost unique" in the sense that the elements of G that have an ambiguous representation of this type lie on certain lower dimensional submanifolds in G. Since U commutes with the T_i, a general SU(3) matrix in the form

$$W = e^{3idU}\, e^{2i\vec{a}\cdot\vec{T}}\, e^{i(nN + n'N' + mM + m'M')}. \qquad (6.50)$$

Using Hausdorff's theorem (29) and making appropriate redefinitions of the parameters, this can be written in the form

$$W = e^{3idU}\, e^{2i\vec{a}\cdot\vec{T}}\, e^{3idU}\, e^{inN}\, e^{2i\vec{a}'\cdot\vec{T}} \qquad (6.51)$$

$$= e^{3idU}\, e^{2i\vec{a}\cdot\vec{T}}\, e^{inN}\, e^{2i\vec{a}'\cdot\vec{T}}\, e^{3idU},$$

where use has been made of the relation

$$e^{ibU}\, e^{inN}\, e^{-ibU} = e^{2ibT_3}\, e^{inN}\, e^{-2ibT_3}\ .$$

Since we are considering only the subset of SU(3) matrices containing the symmetric matrices (from time-reversal invariance of the S-matrix), we can write

$$W = S' \cdot e^{2i\vec{a}'\cdot\vec{T}}\ , \tag{6.52}$$

where

$$S' = e^{3idU}\, e^{2i\vec{a}\cdot\vec{T}}\, e^{inN}\, \{e^{2i\vec{a}\cdot\vec{T}}\}_{\text{transpose}}\, e^{3idU}. \tag{6.53}$$

A general unitary, symmetric 3X3 matrix depends on six parameters and can be written in the form

$$S = e^{2ie}\cdot S' \tag{6.54}$$
$$= e^{2ie}\,(e^{3idU}\, e^{2iaT_3}\, e^{2ibT_2}\, e^{2icT_3}\, e^{inN}\, e^{2icT_3}\, e^{-2ibT_2}\, e^{2iaT_3}\, e^{3idU}),$$

since T_3, U and N are symmetric and T_2 is antisymmetric. Doing the indicated operations, we obtain for the matrix elements of S the following:

$$S_{11} = e^{2ie}\, e^{2i(d+a)}\,(\cos^2 b\, \cos n\, e^{2ic} + \sin^2 b\, e^{-2ic}) \tag{6.55}$$

$$S_{12} = e^{2ie}\,(-\sin b \cos b\, e^{2id})\ (\cos n\, e^{2ic} - e^{-2ic})$$

$$S_{13} = e^{2ie}\,(i \cos b \sin n\, e^{-i(d-a+c)})$$

$$S_{22} = e^{2ie}\, e^{2i(d-a)}\,(\sin^2 b \cos n\, e^{2ic} + \cos^2 b\, e^{-2ic})$$

$$S_{23} = e^{2ie}\,(-i \sin b \sin n\, e^{-i(d+a+c)})$$

$$S_{33} = e^{2ie} \cos n\, e^{-4id}.$$

Since an elastic scattering amplitude can be parameterized in terms of a two-parameter complex phase shift, we want to relate the matrix S in 6.54 to a matrix of the form

$$S = \begin{Bmatrix} re^{2id_1} & ue^{i(d_1+d_2+x)} & ve^{i(d_1+d_3+y)} \\ \cdots & se^{2id_2} & we^{i(d_2+d_3+z)} \\ \cdots & \cdots & te^{2id_3} \end{Bmatrix}, \qquad (6.56)$$

where the complex phase shift δ_i has been put into the form $\delta_i = d_i + i\alpha_i$, $i = 1, 2, 3$, and the inelasticity parameters r, s, and t, are given by $r = e^{-2\alpha_1}$, $s = e^{-2\alpha_2}$, and $t = e^{-2\alpha_3}$. From these definitions and the restriction that α_i be positive or zero, we find the restriction

$0 \leq r, s, t \leq 1$.

The partial wave subscript $\ell\pm$ has been omitted on all the parameters for simplicity.

Comparing 6.56 with 6.55, we can immediately identify

$$t = \cos n, \qquad (6.57)$$

$$d_3 = e - 2d.$$

Manipulating the other two diagonal terms, we obtain the relations

$$\cos 2b = (r^2 - s^2)/(t^2 - 1), \qquad (6.58)$$

$$|u|^2 = \tfrac{1}{2}(1 - r^2 - s^2 + t^2),$$

$$|v|^2 = \tfrac{1}{2}(1 - r^2 + s^2 - t^2),$$

$$|w|^2 = \tfrac{1}{2}(1 + r^2 - s^2 - t^2).$$

Unitarity and symmetry of S require that

$$S_{ij}^{*} = \text{cofactor } S_{ij} / \det S,$$

which gives

$$w^2 = (st\, e^{2i(d_2+d_3)} - r\, e^{2i(e-d_1)}) \cdot e^{-2i(d_2+d_3+z)}. \qquad (6.59)$$

Let $f = e - d_1 - d_2 - d_3$. Then 6.59 can be written

$$w^2 = (st - r\, e^{2if})\, e^{-2iz}. \qquad (6.60)$$

By combining equations 6.58 and 6.60, we obtain an equation for cos 2f,

$$\frac{1}{2}(1 + r^2 - s^2 - t^2)^2 = s^2 t^2 + r^2 - 2rst \cos 2f, \tag{6.61}$$

which leads to

$$\cos 2f = \frac{(1 + r^4 + s^4 + t^4 - 2r^2s^2 - 2r^2t^2 - 2s^2t^2 - 2r^2 - 2s^2 - 2t^2)}{-8rst}. \tag{6.62}$$

It should be noted that the equation for the physical boundary of the inelasticity parameters, r, s, and t, is given by the restriction $-1 \leq \cos 2f \leq +1$. We can now define z in terms of f,

$$\tan 2z = \frac{r \sin 2f}{r \cos 2f - st}. \tag{6.63}$$

Similar manipulations with the other variables in 6.58 give

$$\tan 2x = \frac{t \sin 2f}{t \cos 2f - rs}, \tag{6.64}$$

and

$$\tan 2y = \frac{s \sin 2f}{s \cos 2f - rt}. \tag{6.65}$$

The usual condition for a resonance to appear in the elastic channel is that the real part of the phase shift pass through $\frac{\pi}{2}$ at that value of energy corresponding to the mass of the resonance, if the resonance in question is an elastic resonance, i. e., a resonance for which $r \geq \frac{1}{2}$ when $d_1 = \frac{\pi}{2}$. For an inelastic resonance (or absorptive resonance), the real part of the phase shift passes through zero at the resonance energy, since in this instance $r < \frac{1}{2}$. In either case, to ensure that these resonances appear in the inelastic channel at the same energy we must require that x, y, and z be multiples of $\frac{\pi}{2}$. This is just the requirement that sin 2f vanish, which implies that $\cos 2f = \pm 1$. For cos 2f = +1, 6.62 becomes

$$(-r + s + t - 1)(r - s + t - 1)(r + s - t - 1)(r + s + t + 1) = 0. \tag{6.66}$$

The condition that connects the 3x3 S-matrix smoothly to the 2x2 S-matrix when the third channel becomes pure elastic (i. e., the third channel decouples from the remaining channels, and t = 1) is

$$r - s + t = 1. \tag{6.67}$$

Unitarity fixes the relative phases of the off-diagonal elements, and the final form for the inelastic processes is

$$S_{12} = \pm i\ (1 - r)^{1/2}(1 + s)^{1/2}\ e^{i(d_1+d_2)}\ , \tag{6.68}$$

$$S_{13} = \mp\ (1 - r)^{1/2}(1 - t)^{1/2}\ e^{i(d_1+d_3)}\ ,$$

$$S_{23} = \pm i\ (1 + s)^{1/2}(1 - t)^{1/2}\ e^{i(d_2+d_3)}.$$

In the limit $t \to 1$, where only two channels are open, these terms go to

$$S_{12} = \pm i\ (1 - r)^{1/2}(1 + r)^{1/2}\ e^{i(d_1+d_2)}\ , \tag{6.69}$$

$$S_{23} = S_{13} = 0,$$

which corresponds to the symmetric unitary 2x2 matrix.

The scattering amplitude T is given by

$$T = (1 - S)/2i\ , \tag{6.70}$$

$$T_{11} = -\frac{1}{2}\, r \sin 2d_1 - \frac{1}{2}\, i(1 - r\cos 2d_1), \tag{6.71}$$

$$T_{12} = -\frac{1}{2}\,(1 - r)^{1/2}(1 + s)^{1/2}\,[\cos(d_1+d_2) + i \sin(d_1+d_2)]. \tag{6.72}$$

In this representation, a resonance appearing simultaneously (as a function of energy) in the elastic channels 1 and 2 causes the diagonal elements to become pure imaginary, as in 6.71 for $d_1 = \frac{\pi}{2}$ or 0, and the off-diagonal elements to become pure real, as in 6.72 when both d_1 and d_2 are equal to $\frac{\pi}{2}$ or 0.

An Argand diagram is a plot of Real $T_{\ell\pm}$ versus Imaginary $T_{\ell\pm}$ as a

function of energy. The Argand diagrams for the elastic amplitude, 6.71, and the inelastic amplitude, 6.72, are shown in Fig. 11. Below the inelastic threshold, r = s = 1; the phase shifts are zero at the threshold for the reaction, and increase with energy, passing through $\frac{\pi}{2}$ at the resonance energy. The case depicted in Fig. 11 is that of a purely elastic resonance for which r = 1 for all energies, and the Argand diagram describes the unitary circle. Amplitudes which include some effects of non-resonating background or inelastic thresholds would be expected to exhibit more intricate structure, such as loops reflecting variations of the inelasticity parameter. Some of this type structure may be seen in the diagrams in Fig. 6.

As is evident from 6.68, the overall phase of the inelastic amplitude is arbitrary up to a factor $e^{i\pi/2}$. This means that the diagram in Fig. 11 for the inelastic amplitude can be rotated about the origin by multiples of $\frac{\pi}{2}$. In the Argand diagrams calculated in Chapter V, an example of which is shown in Fig. 6, the diagrams for $T_{j=\ell+1/2}$ appear to be out of phase by π radians with the diagrams for $T_{j=\ell-1/2}$, corresponding to the $\pm$ sign ambiguity in the matrix element S_{12} in 6.68.

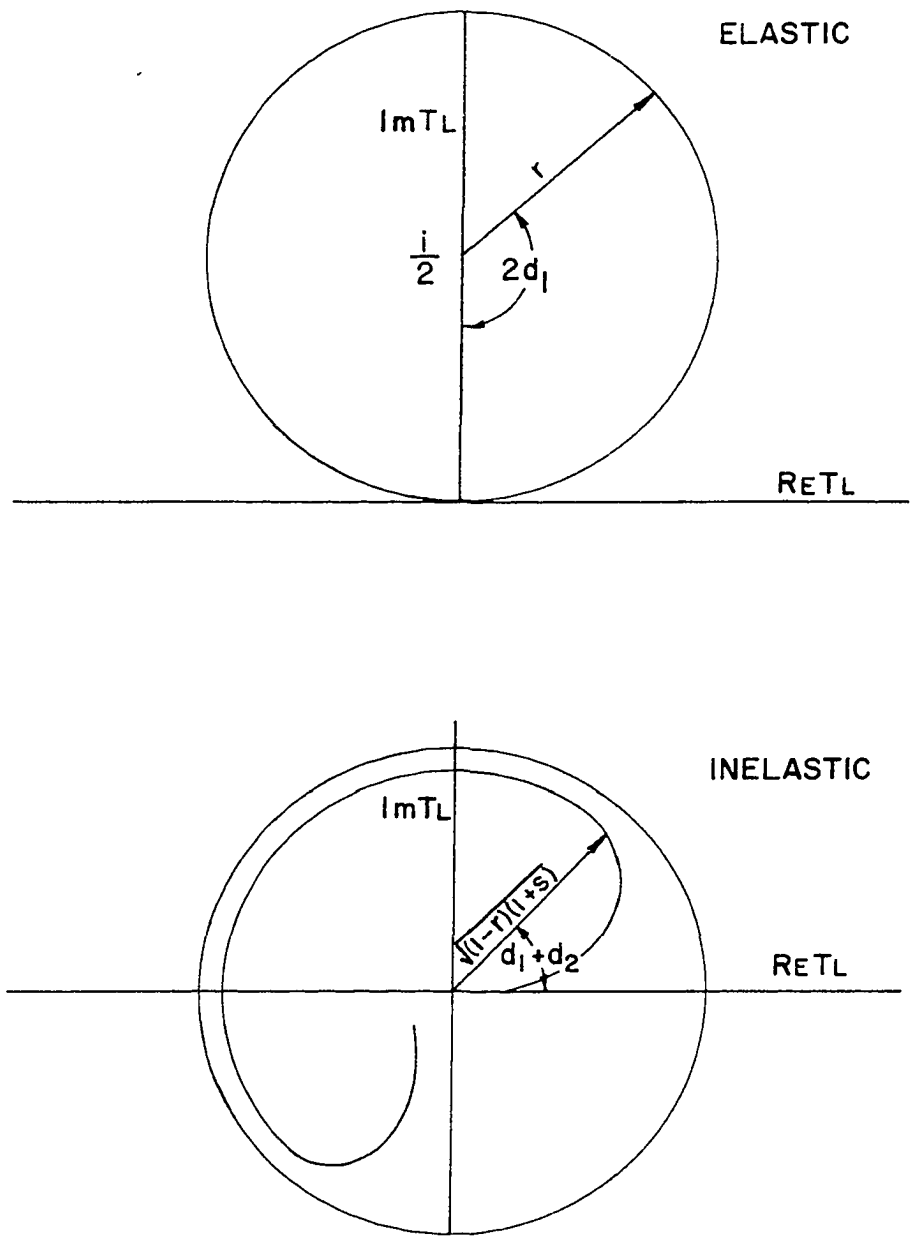

Fig. 11. Argand Diagrams for Resonance Amplitudes in the Elastic and Inelastic Channels

VII. LITERATURE CITED

1. Gell-Mann, M. and Ne'eman, Y., The Eightfold Way, W. A. Benjamin, Inc., New York, 1964.

2. Bjorken, J. D. and Drell, S. D., Relativistic Quantum Fields, McGraw-Hill, Inc., New York, 1965.

3. Coleman, S. and Schnitzer, H. T., Phys. Rev. 134, B863 (1964).

4. Rivers, R. J., Phys. Rev. 150, 1256 (1966).

5.a. Chikovani, G., Focacci, M. N., Kienzle, W., Lechanoine, C., Levrat, B., Maglic, B., Martin, M., Schübelin, P., Dubal, L., Fischer, M., Greider, P., Neal, M. A. and Nef, C., Phys. Letters 25B, 44 (1967).

5.b. Benz, H., Chikovani, G. C., Damgaard, G., Focacci, M. N., Kienzle, W., Lechanoine, C., Martin, M., Nef, C., Schübelin, P., Baud, R., Bosnjakovic, B., Cotteron, J., Klanner, R. and Weitsch, A., Phys. Letters 28B, 233 (1968).

5.c. Crennell, D. J., Karshon, V., Lai, K. W., Scarr, J. M. and Skillicorn, I. O., Phys. Rev. Letters 20, 1318 (1968).

6. Austin, D. M., Beaupre, J. V. and Lassila, K. E., Phys. Rev. 173, 1573 (1968).

7. DiVecchia, P., Drago, F., Ferro Fontan, C. and Odorico, R., Trieste Preprint IC/68/67 (1968); DiVecchia, P., Drago, F., Ferro Fontan, C., Odorico, R. and Paciello, M. L., Trieste Preprint IC/68/40 (1968).

8. Elitzen, M., Rubinstein, H. R., Stern, H. and Lipkin, H. J., Phys. Rev. Letters 17, 420 (1966); Horn, D., Lipkin, H. J. and Meshkov, S., Phys. Rev. Letters 17, 1200 (1966).

9. McNamee, P. and Chilton, F., Rev. Mod. Phys. 36, 1005 (1964).

10. Lassila, K. E. and Ruuskanen, P. V., Phys. Rev. Letters 19, 762 (1967); Beaupre, J. V., Coleman, T. P., Lassila, K. E. and Ruuskanen, P. V., Phys. Rev. Letters 21, 1849 (1968).

11. Resnikoff, M. and Silbar, R. R., Phys. Rev. 149, 1256 (1966); Resnikoff, M. and Silbar, R. R., Phys. Rev. 159, 1510 (1967).

12. Vanderhage, R., Huc, J., Fleury, P., Duboc, J., George, R., Goldberg, M., Makowski, B., Armenise, N., Ghidini, B., Picciarelli, V., Romano, A., Forino, A., Gessaroli, R., Quareni, G. and Quareni-Vignudelli, A., Phys. Letters 24B, 493 (1967); Fiorini, E., Meson Resonances, in Zichichi, A., Ed., 1966 International School of Physics "Ettore Majorana," pp. 378-467, Academic Press, New York, 1966.

13. Eden, R. J., High Energy Collisions of Elementary Particles, Cambridge University Press, Cambridge, England, 1967.

14. Gell-Mann, M., Goldberger, M. L., Low, F. E., Marx, E. and Zachariasen, F., Phys. Rev. 133, B145 (1964).

15. Wang, L.L.C., Phys. Rev. 142, 1187 (1966); Wang, L.L.C., Phys. Rev. 153, 1664 (1967).

16. Jacob, M. and Wick, G. C., Annals of Physics, 7, 404 (1959).

17.a. Guisan, O., Kirz, J., Sonderegger, P., Stirling, A. V., Borgeaud, P., Bruneton, C., Falk-Vairant, P., Amblard, B., Caversasio, C., Guillaud, J. P. and Yvert, M., Phys. Letters 18, 200 (1965).

17.b. Drubnis, D. D., Lales, J., Lamb, R. C., Lundy, R. A., Morretti, A., Niemann, R. C., Novey, T. B., Simanton, J., Yokosawa, A. and Yovanovitch, D., Phys. Rev. Letters 20, 274 (1968).

17.c. Bulos, F., Lanou, R. E., Pifer, A. E., Shapiro, A. M., Widgoff, M., Brenner, A. E., Bordner, C. A., Law, M. E., Ronat, E. E., Strauch, K., Szymanski, J. J., Bastien, P., Brabson, B. B., Eisenberg, Y., Feld, B. T., Fischer, V. K., Pless, I. A., Rosenson, L., Yamamoto, R. K., Calvelli, G., Guerriero, L., Salandin, G. A., Tomasin, A., Ventura, L., Voci, C. and Waldner, F., Phys. Rev. Letters 13, 486 (1964); Richards, W. B., Chiu, C. B., Eandi, R. D., Helmholz, A. C., Kenney, R. W., Mayer, B. J., Poirier, J. A., Cence, R. J., Peterson, V. Z., Sehgal, N. K., Stenger, V. J., Phys. Rev. Letters 16, 1221 (1966); Carroll, A. S., Corbett, C.J.S., Middlemas, N., Newton, D., Clegg, A. B., and Williams, W.S.C., Study of Neutral Final States Produced in π^- p Collisions at Momenta of 1.71-2.46 GeV/c, Rutherford Preprint, Rutherford, England, 1968.

18. Ball, J. S., Frazer, W. R. and Jacob, M., Phys. Rev. Letters 20, 518 (1968); Bietti, A., DiVecchia, P., Drago, F. and Paciello M. L., Phys. Letters 26B, 457 (1968).

19. Arnold, R. C., Phys. Rev. Letters 14, 657 (1965); Ahmadzadeh, A., Phys. Rev. Letters 20, 1125 (1968).

20. Dolen, R., Horn, D. and Schmid, C., Phys. Rev. 166, 1768 (1968); Schmid, C., Phys. Rev. Letters 20, 689 (1968).

21. Collins, P.D.B., Johnson, R. C. and Squires, E. J., Phys. Letters 27B, 23 (1968).

22. Lovelace, C., Nucleon Resonances in Low Energy Scattering, in Filthuth, H., Ed., Proceedings of the Heidelberg International Conference on Elementary Particles, pp. 79-116, John Wiley and Sons, Inc., New York, 1968.

23. Alessandrini, V. A., Freund, P.G.O., Oehme, R. and Squires, E. J., Phys. Letters 27B, 456 (1968).

24. Ademollo, M., Rubenstein, H. R., Veneziano, G. and Virasoro, M. A., Phys. Rev. Letters 19, 1402 (1967); Rubenstein, H. R., Schwimmer, A., Veneziano, G. and Virasoro, M. A., Phys. Rev. Letters 21, 491 (1968).

25. Bertocchi, L., Theoretical Aspects of High Energy Phenomenology, in Filthuth, H., Ed., Proceedings of the Heidelberg International Conference on Elementary Particles, pp. 197-252, John Wiley and Sons, Inc., New York, 1968.

26. Arbab, F., Bali, N. F. and Dash, J. N., Phys. Rev. 158, 1515 (1967).

27. Gasiorowicz, S., Elementary Particle Physics, John Wiley and Sons, Inc., New York, 1966.

28. Chew, G. F., Goldberger, M. L., Low, F. E. and Nambu, Y., Phys. Rev. 106, 1337 (1957).

29. Nelson, T. J., J. Math. Phys. 8, 857 (1967).

30. Hermann, R., Lie Groups for Physicists, John Wiley and Sons, Inc., New York, 1966.

VIII. ACKNOWLEDGMENTS

The author gratefully acknowledges the kind assistance of Prof. K. E. Lassila who suggested this problem and provided many useful discussions. He would also like to thank Dr. J. V. Beaupre and Mr. D. Zacrep for their assistance with the computer programming, and Dr. W. H. Greiman for his assistance with the group theory.